Oral Cavity and Oropharynx

4

Sugoto Mukherjee, Brian M. Trotta, Mark J. Jameson, Max Wintermark, and Prashant Raghavan

4.1 Introduction

Squamous cell carcinomas (SCCs) represent the vast majority of lesions in the oral cavity and oropharynx (OC/OP). The imaging appearance of these cancers and their common pathways of spread are the focus of this chapter, and a few of the other lesions of the OC/OP are reviewed.

4.2 Anatomy

The oral cavity is separated from the sinonasal region by the hard and soft palate and from the oropharynx by the circumvallate papilla of the tongue, soft palate, and anterior tonsillar pillars (Fig. 4.1). The maxillary tuberosity serves as the radiographic border between the oral cavity and oropharynx.

From an imaging standpoint, the oral cavity can be subdivided into four distinct regions: (1) the oral mucosal surface, including the floor of mouth; (2) the root of the tongue; (3) the sublingual space; and (4) the submandibular space (Fig. 4.2). All the surfaces of the oral cavity structures are covered with keratinizing stratified squamous epithelium along with minor salivary gland rests.

The tongue is divided into an oral part (anterior two-thirds within the oral cavity), the base (posterior one-third within the oropharynx), and the root. The circumvallate papilla of the tongue separates the oral tongue from the base of tongue, which also includes the lingual tonsils. The tongue consists of extrinsic muscles (genioglossus, hyoglossus, styloglossus, and palatoglossus), which predominantly move the tongue body, and the intrinsic muscles (superior and inferior longitudinal, transverse, and vertical muscles), which alter tongue shape during swallowing and speech. The root of the tongue consists of the genioglossus-geniohyoid complex and the lingual septum; it extends from the extrinsic tongue muscles superiorly to the mylohyoid sling inferiorly (Fig. 4.3). The vasculature of the tongue consists of the lingual artery (second branch of external carotid) and corresponding lingual vein within the sublingual space. The hypoglossal nerve provides the motor supply and enters the

P. Raghavan et al., *Manual of Head and Neck Imaging*,
DOI 10.1007/978-3-642-40377-4_4, © Springer-Verlag Berlin Heidelberg 2014

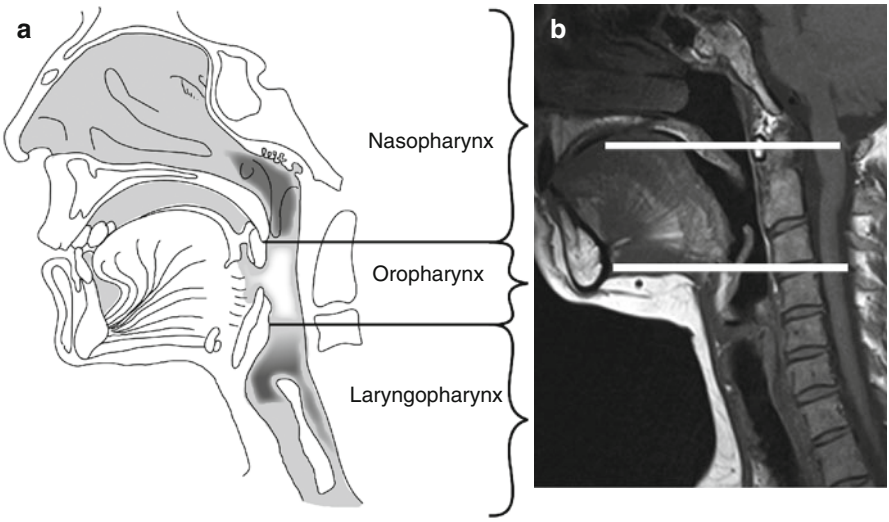

Fig. 4.1 Sagittal graphic (**a**) showing the anatomical landmarks of the oropharynx in between the nasopharynx and laryngopharynx. The oropharynx lies. It is the area in between the hard/soft palate and the pharyngo-epiglottic folds at the level of the inferior epiglottis, marked by the two *horizontal white lines* on the sagittal MR image (**b**)

sublingual space just lateral to the posterior hyoglossus. Sensory supply for the anterior two-thirds is by the lingual nerve, while the posterior one-thirds is supplied by branches from glossopharyngeal nerve (CN IX). The chorda tympani nerve, a branch from the facial nerve (CN VII), carries the taste fibers from the anterior two-thirds within the lingual nerve. All these run in the sublingual space (Fig. 4.2).

The floor of the mouth includes the mylohyoid muscle, the hyoglossus muscle, and the sublingual space, which is located between these two muscles (Fig. 4.2). The sublingual space is a horizontal horseshoe-shaped space deep to the oral tongue that communicates posteriorly within the submandibular space and the inferior parapharyngeal space. It lies in between the mylohyoid muscle inferolaterally and the genioglossus muscle medially. The contents of the sublingual space include the lingual artery and vein, distal segments of CNs IX and X, the lingual nerve containing sensory fibers from CN V3 (mandibular branch of trigeminal) as well as taste fibers through the chorda tympani from CN VII (facial), the sublingual gland and ducts, the deep portion of the submandibular gland, and the submandibular duct.

The submandibular space is a vertical horseshoe-shaped space, inferolateral to the mylohyoid muscle and superior to the hyoid bone. It communicates both with the inferior parapharyngeal space and the posterior aspect of the sublingual space. The submandibular space contains the larger superficial portion of the submandibular gland, anterior belly of the digastric, the facial vein and artery, the inferior loop of the hypoglossal nerve (CN XII), and the submental and submandibular lymph node groups (Fig. 4.2).

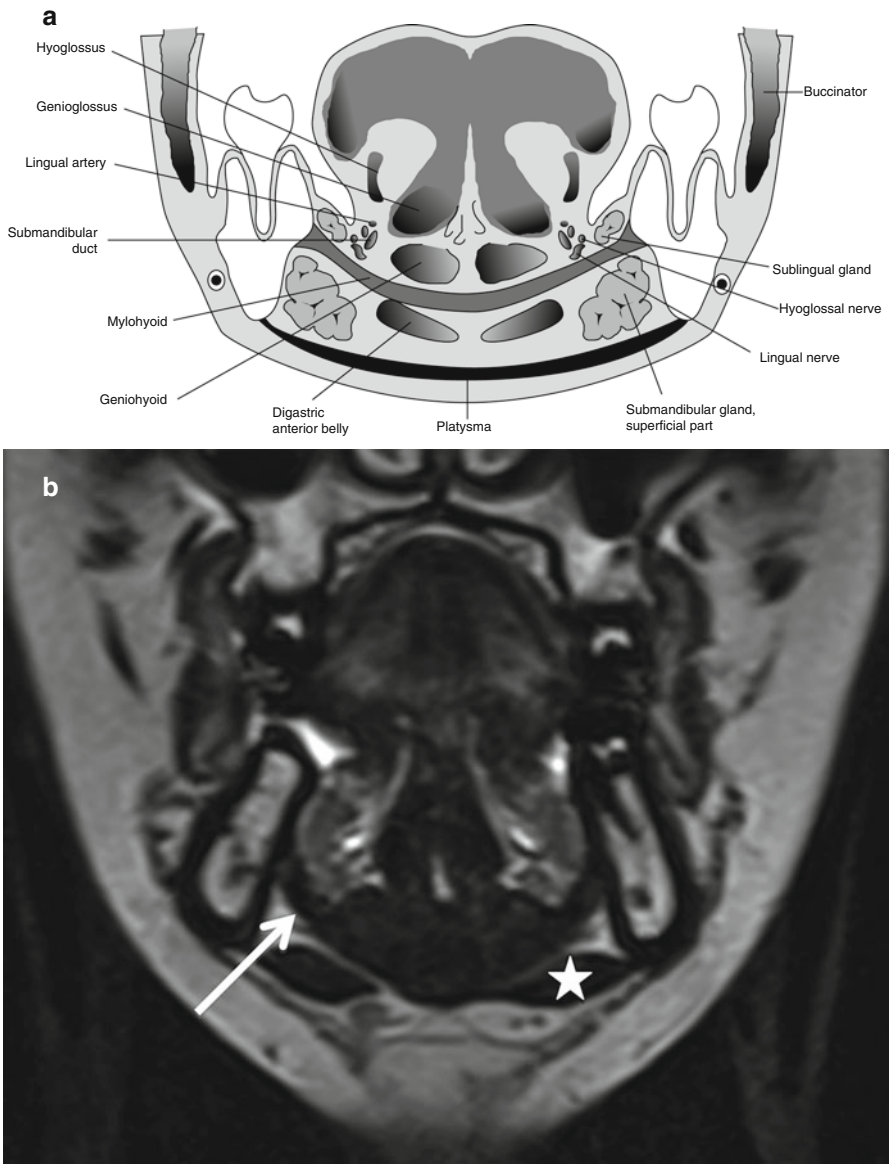

Fig. 4.2 Coronal graphic (**a**) shows the relationship of the sublingual and the submandibular spaces with the mylohyoid muscle. Also note the neurovascular pedicle (consisting of lingual artery and vein, lingual nerve) within the sublingual space. The hypoglossal nerve courses both in the posterior submandibular and sublingual spaces and runs along the surface of hyoglossus muscle before terminating within the tongue. Coronal MR (**b**) shows the mylohyoid muscle as a dark curvilinear sling (*arrow*)-like structure separating the upper sublingual and the inferior submandibular spaces. Also note the paired anterior belly of digastric below the mylohyoid (*star*)

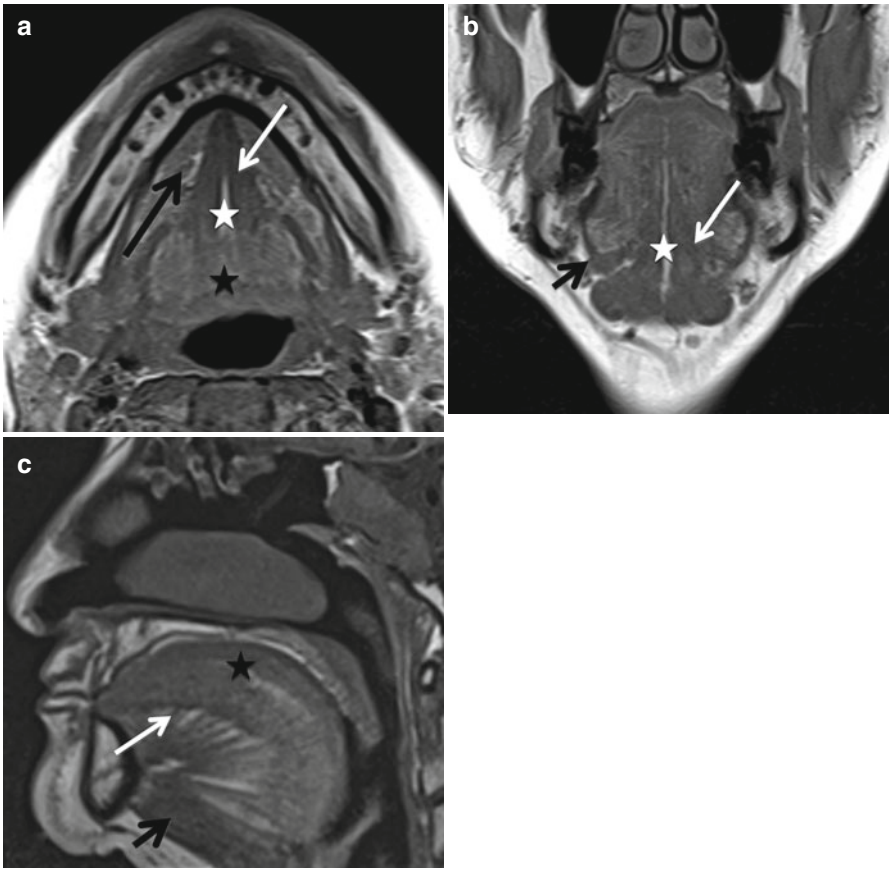

Fig. 4.3 Tongue anatomy is elegantly identified on MR images. On axial T1 (**a**), the lingual septum (with linear T1 hyperintense fat within it) (*white star*), the adjacent genioglossus muscles (*white arrow*), and the intrinsic muscles (*black star*) which are posterior to it. Also note the sublingual spaces lateral to the genioglossus (*long black arrow*). Coronal T1 (**b**) images also show the lingual septum (*white star*), genioglossus as well as the mylohyoid (*short black arrow*). Finally, sagittal T1 (**c**) images show the characteristic fan-like shape of the genioglossus (*white arrow*) along with the geniohyoid and mylohyoid muscles inferiorly (*short black arrow*). The intrinsic tongue muscles are superior to the genioglossus on this sagittal image

The oropharynx includes the posterior third of tongue (base of tongue), the vallecula, the palatine tonsils and tonsillar fossa, the soft palate, the uvula, and the posterior and lateral pharyngeal walls from the soft palate superiorly to the pharyngo-epiglottic folds inferiorly (Fig. 4.1).

Regional nodal metastasis from oral cavity and base of tongue cancers commonly occurs to the submental, submandibular, and upper and mid-cervical lymph chains (levels I–III); for tonsil and pharyngeal wall cancers, regional metastases rarely involve level I.

4.3 Squamous Cell Carcinoma

The most commonly recognized risk factors for SCCs in the head and neck include long-term overuse of alcohol and tobacco. Recently, human papillomavirus (HPV) has been shown to be responsible for the majority of new oropharyngeal SCCs, with HPV-16 accounting for 90–95 % of such cases. Radiologists should be aware of a unique presentation of HPV-associated oropharyngeal cancers, which have an increased tendency to present with large cystic/necrotic level IIa nodal metastases. Given that they have a tendency to occur in younger nonsmokers, these can easily be misinterpreted as second branchial cleft cysts, resulting in missed diagnosis and/or delayed treatment (Fig. 4.4). While second branchial cleft cysts also present as level IIa cystic lesions, they typically present in the first two decades and, unless infected, appear smooth, well circumscribed, and unilocular without any stranding of surrounding structures and without thick or nodular walls. Thus, the presence of an underlying head and neck primary cancer should always be excluded in a young adult with a newly diagnosed level II neck mass.

4.3.1 Radiographic Staging

As with other head and neck SCCs, OC/OP SCCs are staged using the TNM classification system (Boxes 4.1a and 4.1b). Although much of the staging is accomplished

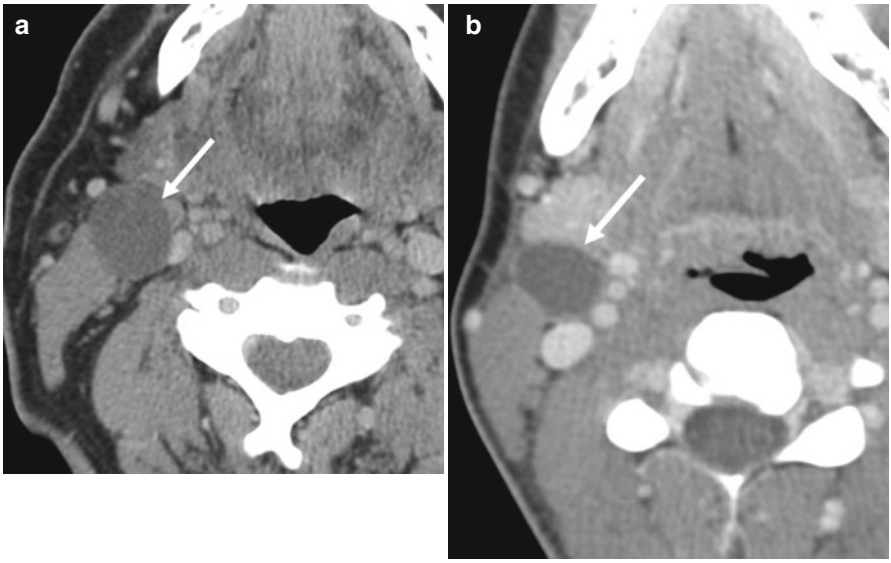

Fig. 4.4 Axial contrast-enhanced CT images from two different patients demonstrate an enlarged fluid density cystic lymph node in a patient with known tonsillar SCC and (*arrow* in **a**) a thin-walled fluid density lesion in the same location in a different patient (*arrow* in **b**) which was found to represent a type II branchial cleft cyst

Box 4.1a. TNM Classification of Squamous Cell Carcinomas of the Oral Cavity and Oropharynx[a]

Disease category	Defining characteristics
	Primary tumor of oral cavity
Tx	Primary tumor cannot be assessed
T0	No evidence of primary tumor is seen
Tis	Primary tumor is carcinoma in situ
T1	Primary carcinoma has a maximal diameter of 2 cm or less
T2	Primary carcinoma has a maximal diameter of 2–4 cm
T3	Primary carcinoma has a maximal diameter of more than 4 cm
T4a	
Lip	Primary tumor invades through cortical bone or involves inferior alveolar nerve, floor of mouth, skin of chin or nose
Oral cavity	Primary tumor invades through cortical bone or involves extrinsic tongue muscles, maxillary sinus, skin of face
T4b	Primary tumor involves masticator space, pterygoid plates, skull base, internal carotid artery
	Primary tumor of oropharynx
Tx	Primary tumor cannot be assessed
T0	No evidence of primary tumor is seen
T1	Primary carcinoma has a maximal diameter of 2 cm or less
T2	Primary carcinoma has a maximal diameter of 2–4 cm
T3	Primary carcinoma has a maximal diameter of more than 4 cm
T4a	Primary tumor involves the larynx, extrinsic muscles of the tongue, medial pterygoid, hard palate, or mandible
T4b	Primary tumor involves the lateral pterygoid muscle, pterygoid plates, lateral nasopharynx, skull base, carotid artery

Modified from Edge SB, Byrd DR, Compton CC et al (eds) (2010) AJCC cancer staging manual, 7th edn. Springer, New York

[a]N and M staging have been covered in Chap. 2

by clinical exam and endoscopy, final staging is heavily dependent upon cross-sectional imaging. Issues of key importance to staging that are clarified or determined by imaging include extent of the primary lesion, invasion of nearby bone, neural and/or vascular involvement, and cervical nodal status, including subclinical cervical nodal metastases and extracapsular spread (ECS) beyond involved nodes. In this process, it is crucial to note involvement of structures that raise concern for resectability (e.g., carotid encasement, pterygoid involvement, skull-base involvement).

4.3.2 Routes of Spread

The general routes of spread of OC/OP SCC are the same for all subsites: (a) direct extension over mucosal surfaces, muscle, and bone; (b) lymphatic drainage

Box 4.1b. Oral Cavity and Oropharyngeal Squamous Cell Carcinoma Stage Grouping Based on TNM Classification

Cancer stage	T category	N category	M category
0	Tis	N0	M0
I	T1	N0	M0
II	T2	N0	M0
III	T3	N0	M0
III	T1 to T3	N1	M0
IVA	T4a	N0 or N1	M0
	T1 to T4a	N2	M0
IVB	T4b	Any N	M0
	Any T	N3	M0
IVC	Any T	Any N	M1

Modified from Edge SB, Byrd DR, Compton CC et al (eds) (2010) AJCC cancer staging manual, 7th ed. Springer, New York

pathways; and (c) extension along neurovascular bundles. However, the particular subsite of involvement of the oral cavity or oropharynx may dictate routine assessment of certain anatomic structures. The relevant imaging anatomy and the patterns of spread for each primary site are summarized in the Boxes 4.2a and 4.2b.

Box 4.2a. Oral Cavity Subsites

Oral cavity subsite	Imaging anatomy	Imaging patterns of tumor spread
Lip	Most often arises along vermilion border	Laterally: Involvement of skin
	Only infiltrative lesions require imaging	Deep: Involvement of orbicularis oris muscle or osseous involvement of buccal surface of maxillary or mandibular ridge
		Lymphatics: Primarily level I and II lymph nodes
Buccal mucosa and gingiva	Buccal mucosa covers lips and cheeks and is continuous with the buccal aspect of the gingiva of the maxillary and mandibular alveolar ridge	Superficial spread most common along buccinator muscle
	Most commonly occurs on lateral walls	Deep: Osseous involvement of maxilla or mandible
	Continuous with retromolar trigone	Posteriorly: To retromolar trigone and pterygomandibular raphe (see below)
		Superiorly: Paranasal sinuses
		Lymphatics: Primarily level I and II lymph nodes

Oral cavity subsite	Imaging anatomy	Imaging patterns of tumor spread
Retromolar trigone	Triangular-shaped mucosa behind last mandibular molar	Anteriorly: Along alveolar ridge
	Either primary site of SCCA or secondarily involved	Posteriorly: Along masticator space, mandibular ramus, and perineural spread along V3
	Pterygomandibular raphe – fascial band extending from posterior mylohyoid ridge to medial pterygoid hamulus	Superiorly: Along pterygomandibular raphe to medial pterygoid plate
	Provides pathway for tumor spread between buccal, masticator space, and floor of mouth.	Inferiorly: Along pterygomandibular raphe and mylohyoid ridge and muscle.
	Medial pterygoid involvement is heralded clinically by trismus	Also osseous involvement of mandible and perineural spread along inferior alveolar nerve
Floor of the mouth	Crescent-shaped mucosa supported by the mylohyoid, which separates it from the submandibular space	Inferior: Along mylohyoid muscle or along neurovascular bundles
	Divided in half by the lingual frenulum	Anterior and lateral: To gingiva and mandible. Assess for crossing of midline
	Posterior border is tongue and anterior tonsillar pillars	Posteriorly: Along hyoglossus muscle
		Lymphatics: Primarily levels I and II lymph nodes can be bilateral for lesions approaching midline
Oral tongue	Consists of anterior and middle thirds of tongue	Laterally: Along gingiva and mandible. Assess for crossing of midline
	Mostly occur along lateral and ventral surfaces	Inferiorly: Along floor of mouth, intrinsic and extrinsic muscles of the tongue and along neurovascular bundles
		Posteriorly: Along base of tongue and intrinsic/extrinsic muscles of the tongue
		Lymphatics: Primarily levels I and II but regional spread to levels III and IV can occur without involvement of higher levels
Hard palate	Primary SCC of the hard palate is rare	Lateral: Maxillary alveolar ridge
	Most commonly represents direct extension	Superiorly: Into nasal cavity and maxillary sinuses. Perineural spread along greater and lesser palatine nerves which provide pathway to pterygopalatine fossa

Box 4.2b. Oropharyngeal Subsites

Oropharynx subsite	Imaging anatomy	Imaging patterns of tumor spread
Base of the tongue	Extends from circumvallate papillae anteriorly to the vallecula inferiorly	Laterally: Along tonsillar pillars. Assess for crossing of midline Anteriorly: To the sublingual space and oral tongue Posteriorly/Inferiorly: Along intrinsic muscles of the tongue. Under valleculae and into preepiglottic space Lymphatics: Primarily to level II, III, and IV, tongue base has bilateral nodal drainage
Tonsils	Anterior and posterior tonsillar pillars or palatine tonsils Most arise in anterior tonsillar pillar	Superiorly: Along palatoglossus muscle to hard and soft palates. Along tensor and levator palatini muscles and pterygoid muscles. Invasion of nasopharynx and skull base Anteriorly: Along superior constrictor muscles to pterygomandibular raphe (may then involve skull base) Posteriorly: Retropharyngeal or carotid space Inferiorly: Base of tongue Osseous involvement: Primarily pterygoid plates and maxilla Lymphatics: Primarily levels II and III, contralateral involvement higher when HPV related

Evaluation of direct extension is most effectively accomplished by direct visualization, particularly in the case of superficial lesions, but the overall extent of the a tumor is often underestimated by physical examination due to submucosal extension or direct invasion of adjacent structures. The radiologist report should describe in detail the entire extent of the tumor and address all the issues relevant to treatment planning.

4.3.3 Radiographic Evaluation

The key concepts in evaluating oral cavity and oropharyngeal SCCs (Box 4.3) are:

1. *Primary subsite evaluation*: One of the most important concepts in OC/OP carcinoma imaging is to correctly localize the tumor subsite (Fig. 4.5). This helps in accurate description of local tumor extension as well as spread beyond the subsite, e.g., into the adjacent masticator and/or buccal spaces and deep neck structures. Specific features to look for at different subsites include:
   (a) *Lip carcinoma*: Evaluate the depth of soft tissue invasion and look for underlying bony erosion usually along the buccal aspect of maxillary or mandibular ridge (Fig. 4.6). Cases involving the mandible may warrant MRI to assess the inferior alveolar nerve if clinically important.

Box 4.3 Key Imaging Concepts in Oral Cavity/Oropharynx Cancer Imaging

T4 lesions	Know the discriminators for T4 lesions: invasion through cortical bone or involvement of extrinsic tongue muscles, maxillary sinus, facial skin, pterygoid muscles, nasopharynx, skull base, carotid artery, soft tissues of the neck, prevertebral muscles, or larynx
Preepiglottic space	Primary vallecular and BOT tumors can invade the preepiglottic space altering management
Nodal disease	Unilateral or bilateral, size and extracapsular spread
Midline extension	Describe extension of tumor across midline for tongue/BOT/FOM lesions
Spread	Know pathways of tumor spread (see Boxes 4.2a and 4.2b)
Mandible	Mandibular periosteal versus frank cortical involvement
Airway issues	Note should be made of possible airway compromise in larger lesions which would require direct communication and immediate intervention

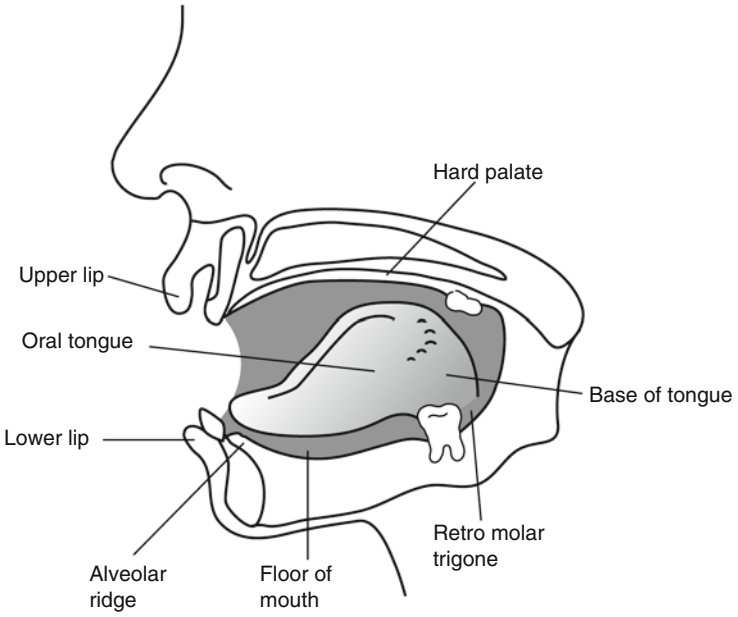

Fig. 4.5 Graphic showing the various subsites of the oral cavity and the oropharynx (base of tongue). Squamous cell carcinomas can arise from any of these subsites. The subsite origin predicts the pattern of cancer spread and consequently affects management and prognosis of these cancers

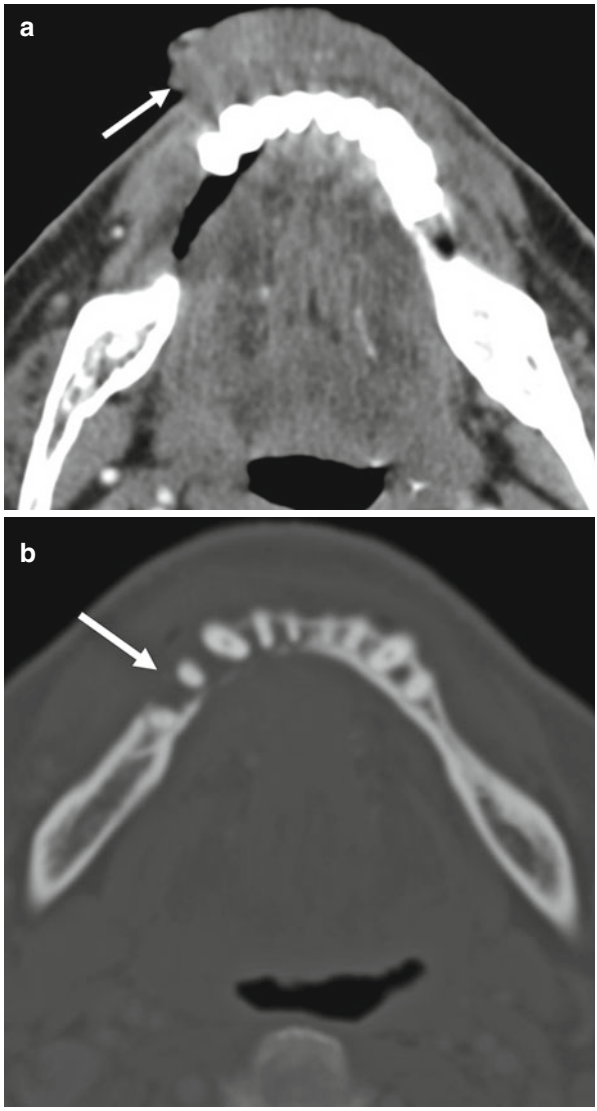

Fig. 4.6 Axial contrast-enhanced CT images in soft tissue and bone windows demonstrate (**a**) a lobulated soft tissue mass arising from the lip which was found to represent SCC and (**b**) cortical destruction of the mandible with loss of normal marrow trabeculae

(b) *Buccal carcinoma*: The primary considerations here are submucosal extension and osseous involvement (Fig. 4.7). On CT, a puffed cheek maneuver may help in identifying smaller lesions (Fig. 4.8).

(c) *Retromolar trigone* (*RMT*) *carcinoma*: Key features to describe are submucosal spread, osseous involvement, and perineural invasion. Often the extent of RMT SCC cannot be determined clinically (Fig. 4.9), regardless of whether the SCC arose primarily from the RMT or represents regional extension of a nearby lesion (Fig. 4.10). Extension along the pterygomandibular raphe allows access to the floor of the mouth.

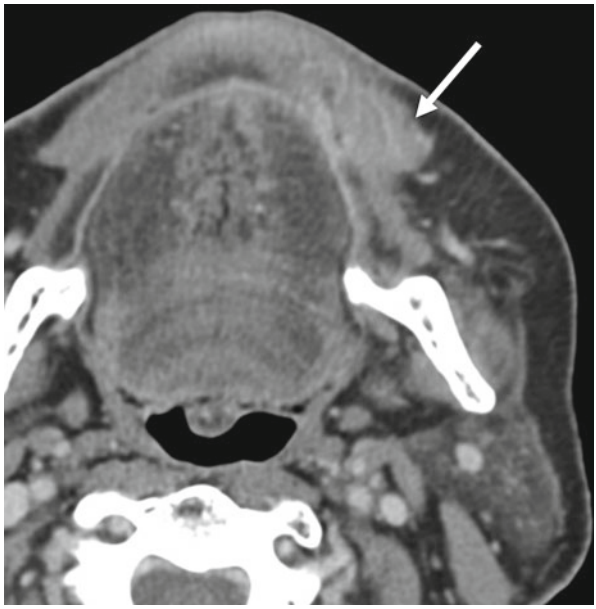

Fig. 4.7 Axial contrast-enhanced CT image demonstrates a soft tissue mass arising from the left buccal mucosa and extending into the adjacent subcutaneous fat, consistent with SCC

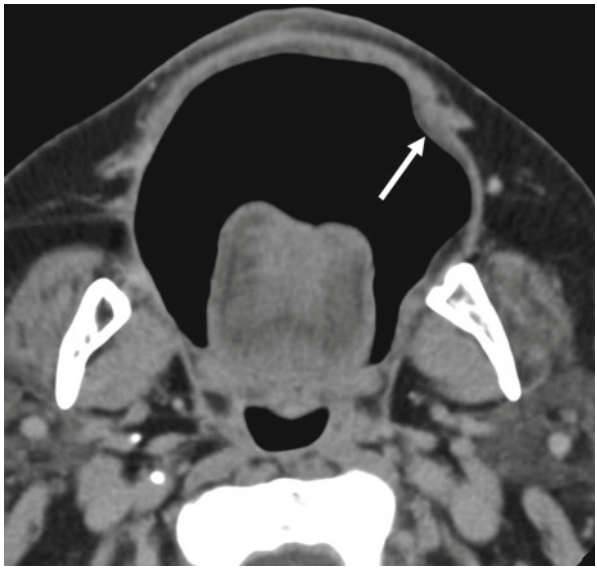

Fig. 4.8 Axial CT image using the "puffed cheek" technique to identify a small SCC arising from the left buccal mucosa (*arrow*). The scan is performed with the patient holding their breath and puffing their cheeks out to increase conspicuity of small lesions

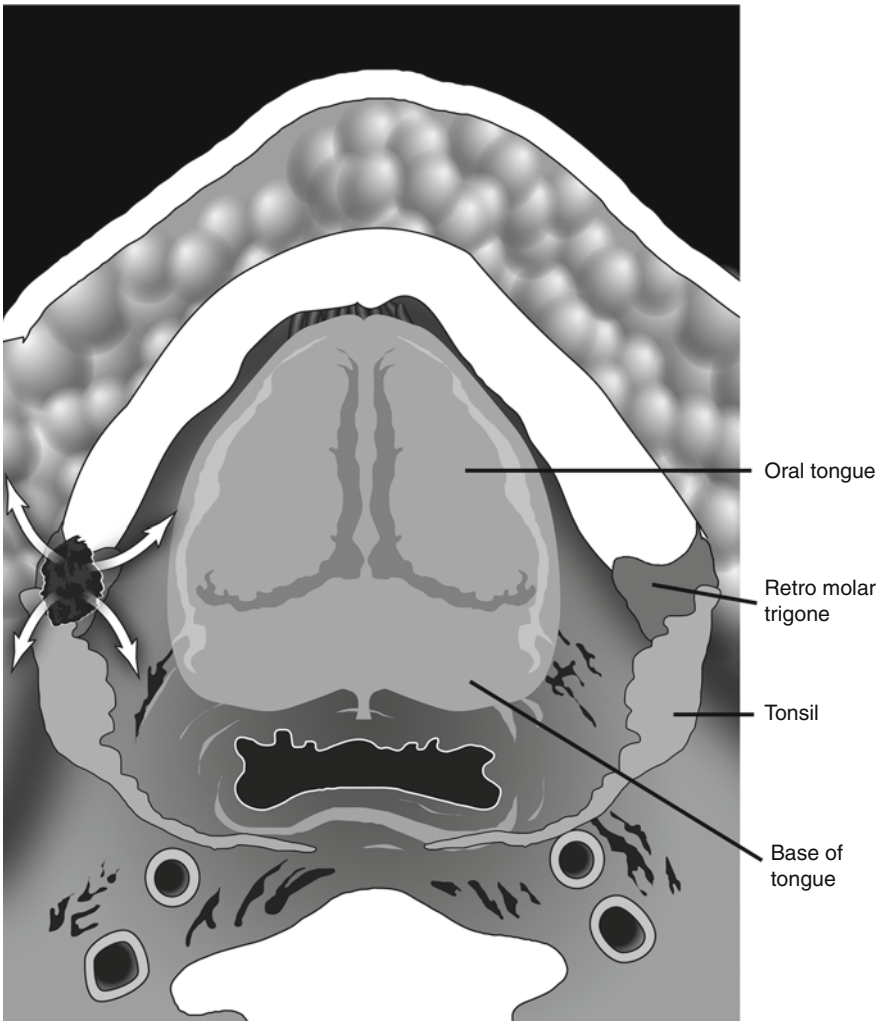

Fig. 4.9 Axial graphic showing normal retromolar trigone (see normal left RMT) situated at the crossroads between oral cavity, oropharynx, masticator space, and buccal space. Consequently, tumor arising in this region, (see right RMT), can spread to all these regions (*white arrows*)

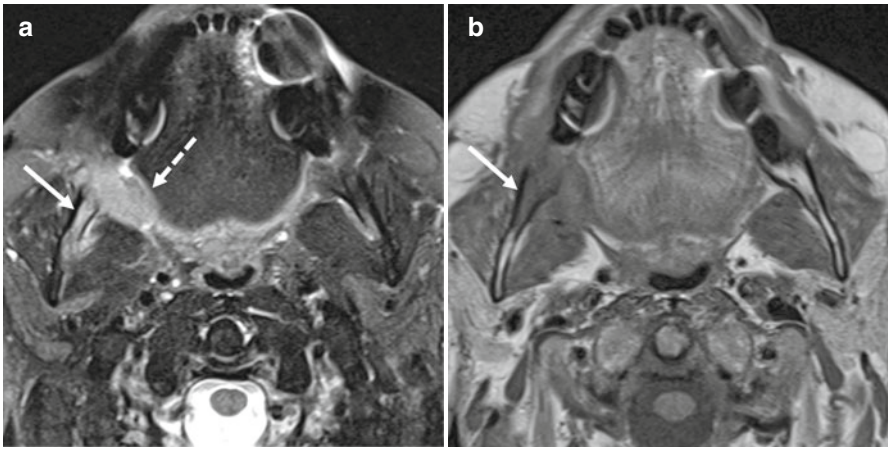

Fig. 4.10 Axial T2-weighted MR image (**a**) with fat saturation demonstrates a T2-hyperintense SCC (*dotted arrow*) arising from the right retromolar trigone with invasion of the mandible (*solid arrow*) as evidenced by abnormal increased T2 signal within the involved bone marrow. Axial T1-weighted image (**b**) of the same patient demonstrates abnormal low T1 signal within the marrow of the right mandible, consistent with osseous invasion

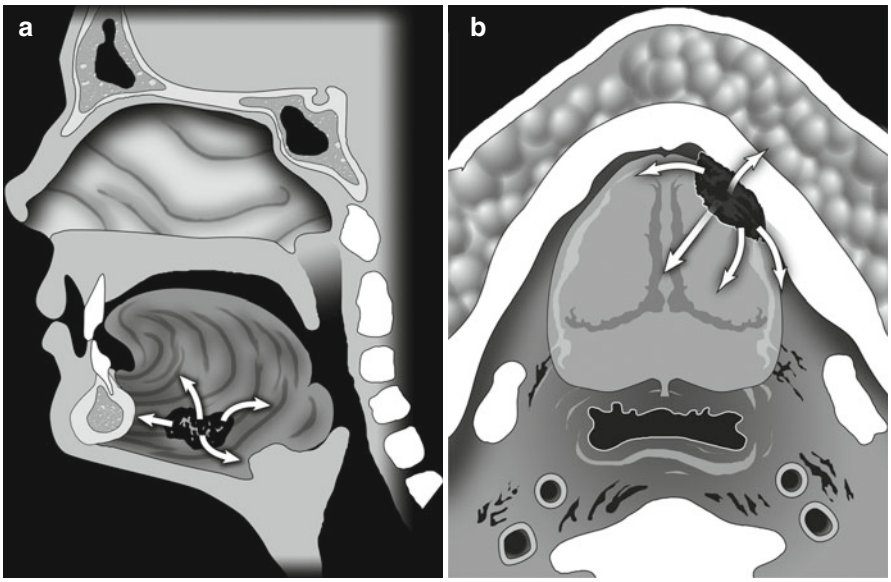

Fig. 4.11 Floor of mouth cancer spread. Sagittal and axial graphic (**a**, **b**) shows the common pathways of spread of a floor of mouth carcinoma into oral tongue, mandible, buccal space, and posteriorly into the base of tongue (*arrows*)

(d) *Floor of mouth* (*FOM*) *carcinoma*: Deep extension along the mylohyoid and hyoglossus muscles should be noted. The relationship to both the ipsilateral and contralateral (if the lesion crosses the midline) neurovascular bundles should be mentioned. Tongue base and osseous invasion must be reported (Figs. 4.11 and 4.12).

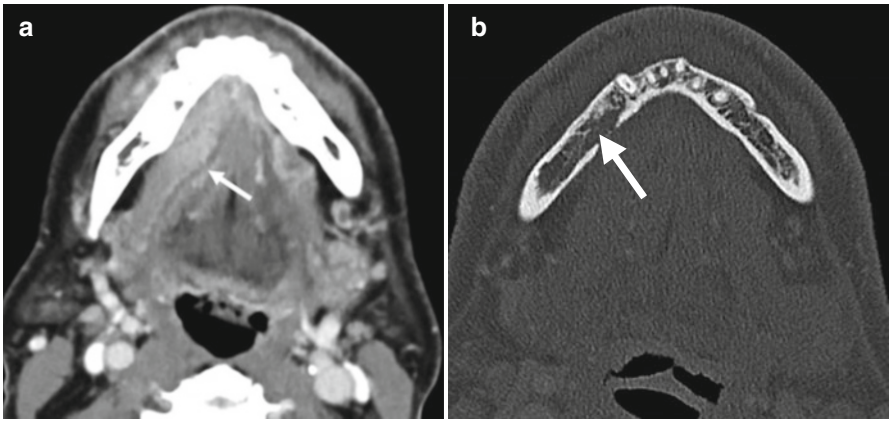

Fig. 4.12 Axial contrast-enhanced CT images in (**a**) soft tissue and (**b**) bone windows demonstrate SCC involving the right floor of the mouth with dilated submandibular duct (*arrow* in **a**) and erosion of the mandibular cortex (*arrow* in **b**)

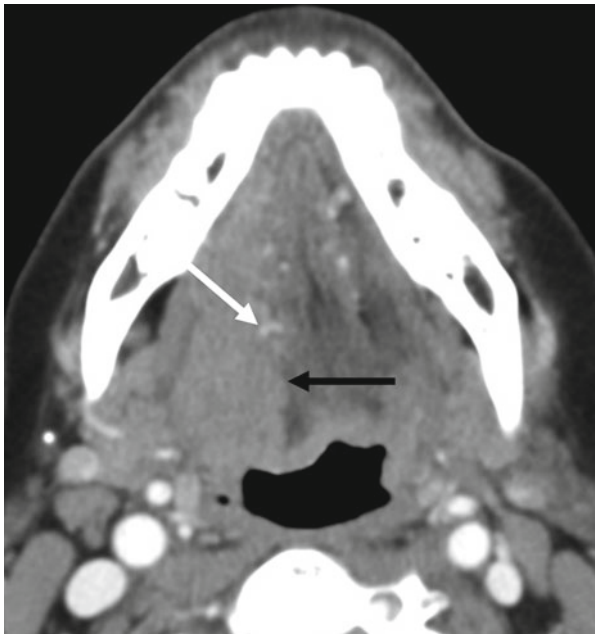

Fig. 4.13 Axial contrast-enhanced CT image in a patient with SCC (*black arrow*) involving the right base of the tongue and oral tongue with involvement of the right lingual neurovascular bundle (*white arrow*). Not that the SCC does not cross the midline of the tongue, an important feature for surgical planning

(e) *Oral tongue*: Note extension across midline, invasion of ipsilateral or contralateral neurovascular bundle, and inferior extension to the floor of mouth (Figs. 4.13, 4.14, and 4.15). Involvement of extrinsic muscles should be mentioned, as these are T4a lesions. Look for osseous involvement of the mandible or perineural extension along the neurovascular bundle.

(f) *Gingiva and hard palate carcinoma*: These rare cancers are best evaluated on coronal and sagittal images due to the axial plane of the hard palate. Bony

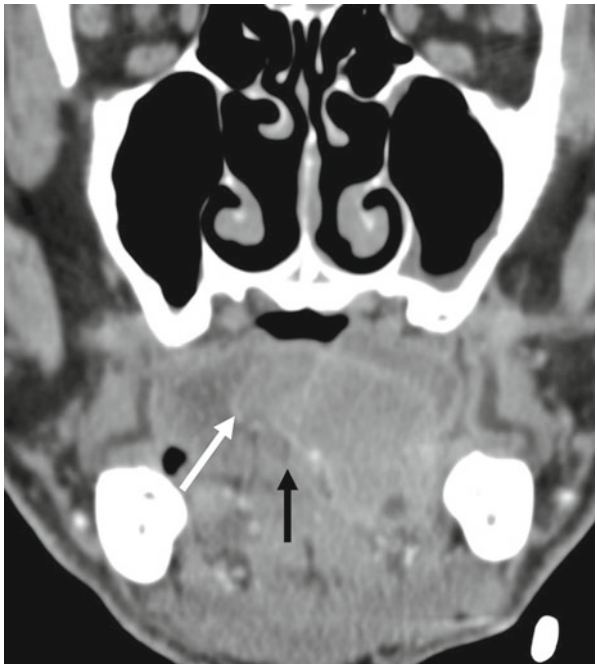

Fig. 4.14 Coronal contrast-enhanced CT image with SCC involving the oral tongue and sublingual space. The left-sided mass crosses to the right of midline (*white arrow*). The *black arrow* indicates the hypodense lingual septum, a useful structure for identifying the midline

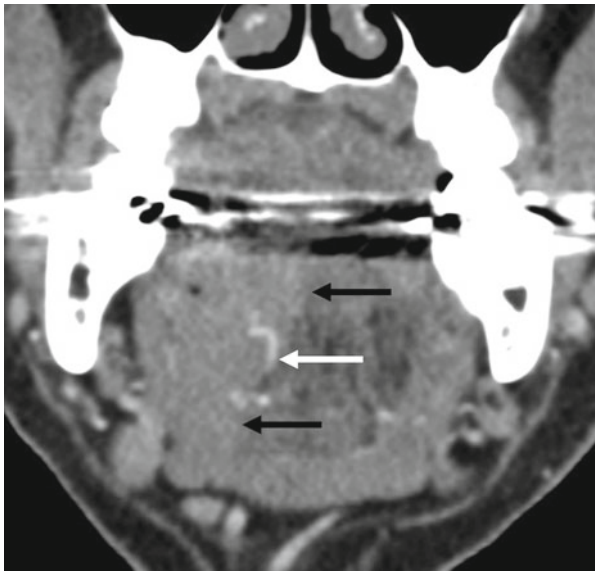

Fig. 4.15 Coronal contrast-enhanced CT image in a patient with SCC (*black arrows*) of the oral tongue and sublingual space with involvement of the lingual neurovascular bundle (*white arrow*)

erosion and perineural invasion of the greater and lesser palatine foramen and the incisive canal are key issues in these cancers (Fig. 4.16).

(g) *Base of tongue* (*BOT*) *carcinoma*: As with FOM SCC, evaluation of the full extent of the tongue involvement is necessary, including extent across midline (Fig. 4.17; *precludes hemiglossectomy*) and involvement of the extrinsic

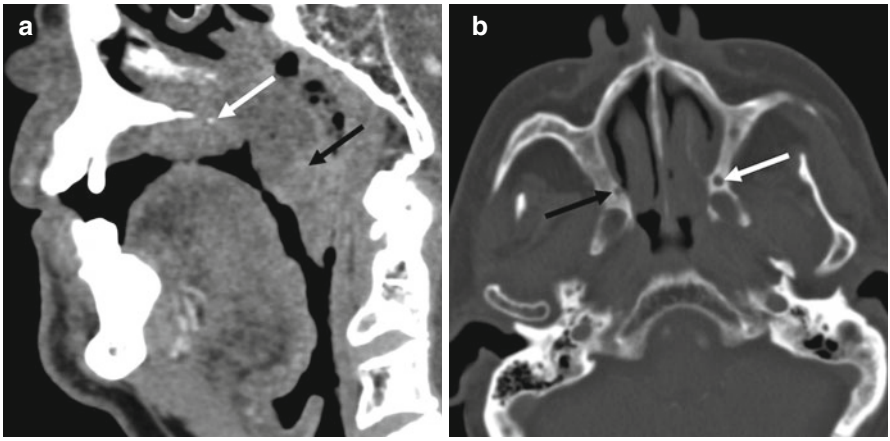

Fig. 4.16 (**a**) Contrast-enhanced sagittal CT image in a patient with SCC involving the soft palate (*black arrow*) with erosion of the hard palate (*white arrow*). (**b**) Axial CT image in the same patient with enlargement and sclerosis of the left greater palatine foramen (*white arrow*) as compared to the normal right greater palatine foramen (*black arrow*) likely indicating perineural spread along the left greater palatine nerve

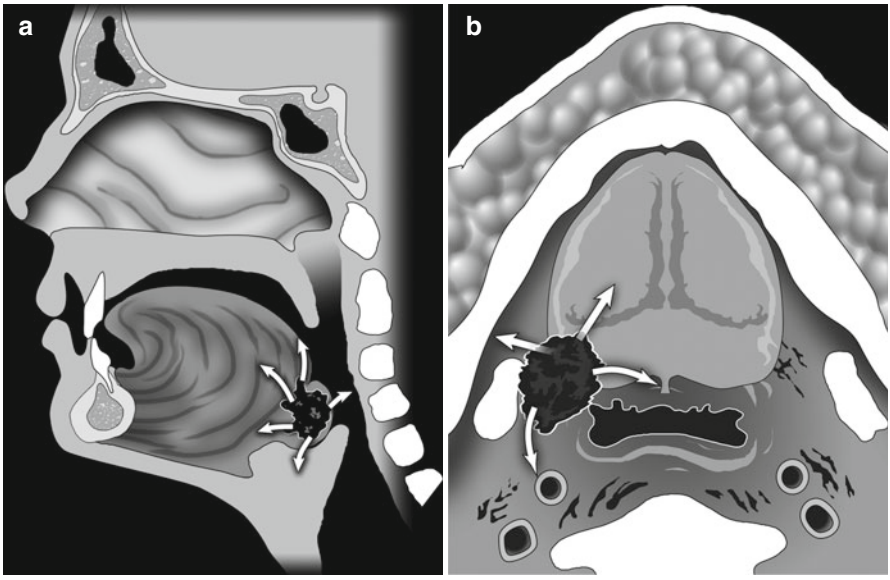

Fig. 4.17 Sagittal (**a**) and axial (**b**) graphic of base of tongue cancer spread. A base of tongue cancer can spread (*arrows*) into oral tongue, floor of mouth, and into the parapharyngeal and carotid paces. Posteriorly, it can extend into the retropharyngeal and prevertebral spaces

musculature (*T4a lesion*; Fig. 4.17). Other features to note include spread to the FOM (including involvement of neurovascular bundle and perineural spread), the anterior tonsillar pillar, and/or the larynx via involvement of the preepiglottic fat (*precludes partial glossectomy*; Figs. 4.17 and 4.18). Axial

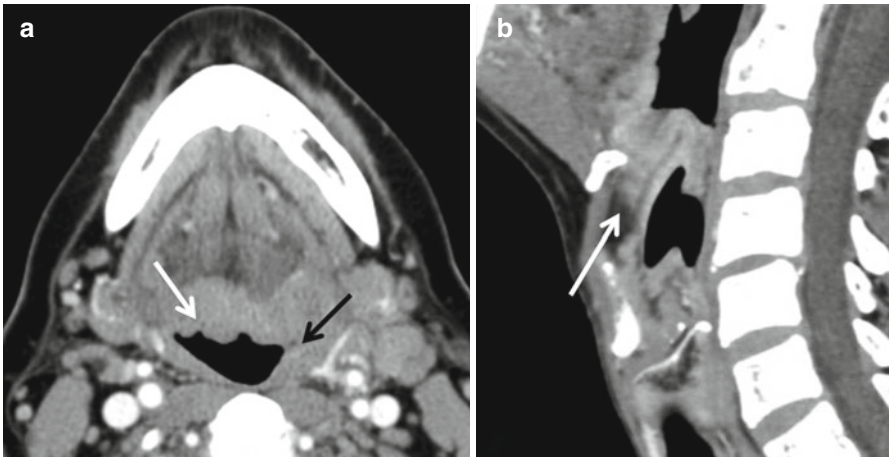

Fig. 4.18 Axial contrast-enhanced CT image (**a**) in a patient with SCC involving the left base of the tongue as well as the entire left side of the oropharynx (*black arrow*). The lesion also crosses the midline of the base of the tongue (*white arrow*). Sagittal CT image (**b**) in the same patient demonstrates tumor anterior to the epiglottis with hazy soft tissue density within the preepiglottic fat, consistent with invasion of the larynx

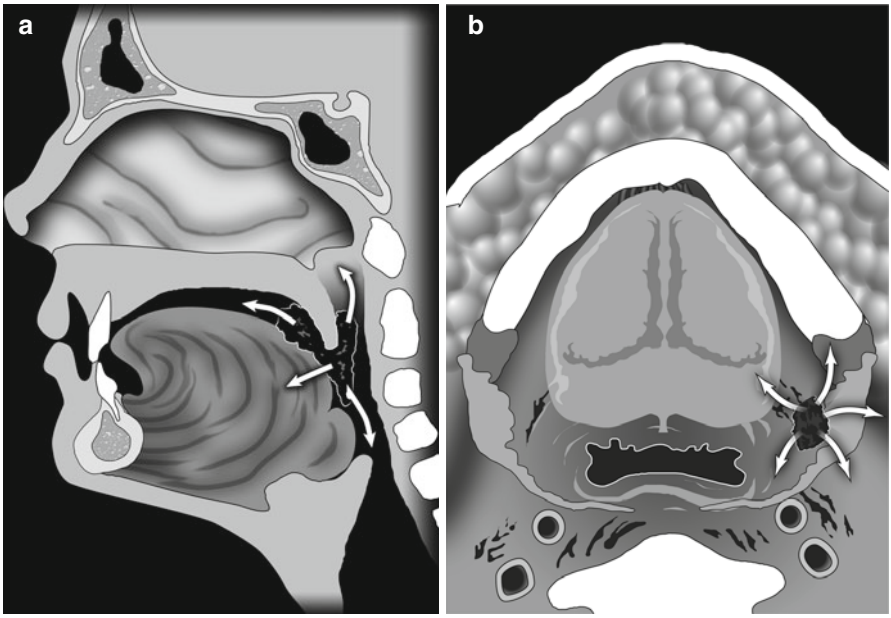

Fig. 4.19 Tonsillar carcinoma spread. Sagittal (**a**) and axial (**b**) graphic shows the common pathways for tonsillar cancer spread into the tongue base, deeper into the parapharyngeal and carotid space, and superiorly and inferiorly along the oropharyngeal walls (*arrows*)

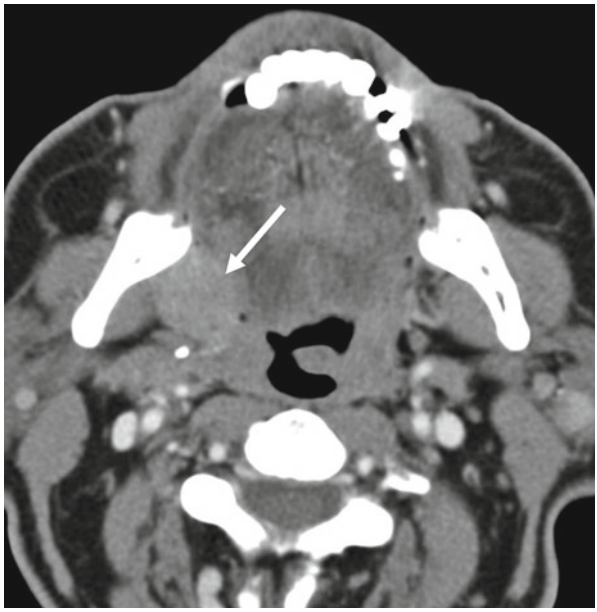

Fig. 4.20 Contrast-enhanced CT image demonstrating SCC arising from the right tonsillar fossa (*arrow*) and involving the right anterior tonsillar pillar

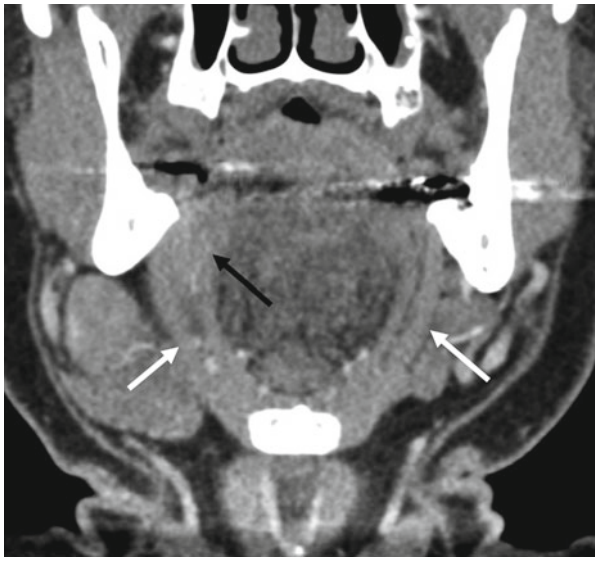

Fig. 4.21 Coronal contrast-enhanced CT image in a patient with right tonsillar SCC (*black arrow*) with loss of the fat plane between the lesion and the mylohyoid muscle, indicating invasion of the mylohyoid muscle and possible extension into the submandibular space

and sagittal T1-weighted MR images are particularly useful in the evaluation of the preepiglottic fat.

(h) *Tonsillar carcinoma*: Describe tongue base invasion and deeper extension into the parapharyngeal space (Figs. 4.19, 4.20, and 4.21). Describe carotid sheath invasion (Fig. 4.22), as well as skull-base, osseous, and prevertebral space involvement (Fig. 4.22). Given that new transoral surgical techniques are

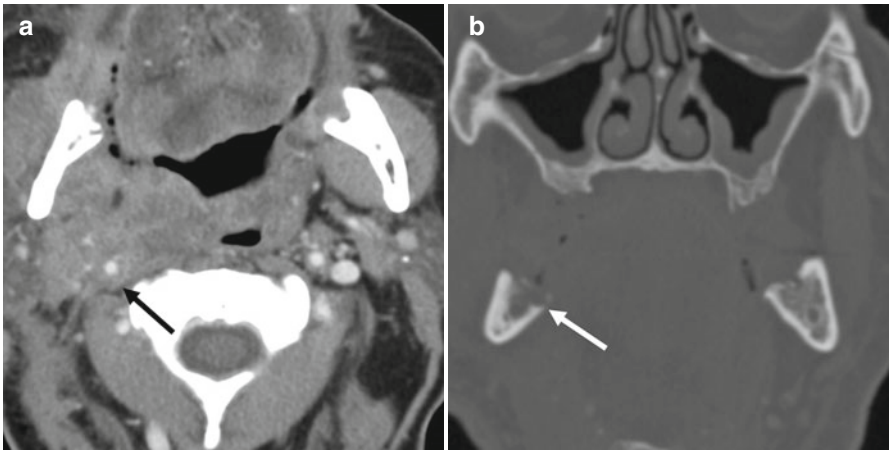

Fig. 4.22 (**a**) Contrast-enhanced axial CT image in a patient with a large right tonsillar SCC which extends to the skull base and encases the right internal carotid artery. (**b**) Coronal CT image in the same patient demonstrates erosion of the adjacent mandibular cortex

contraindicated in the presence of a retropharyngeal carotid artery, the positions of the carotids should be noted whether or not they are involved by cancer.

2. *Osseous involvement*: This includes presence or absence usually of mandibular and, less often, maxillary or palatine involvement. When tumor completely penetrates the bony cortex, all oral cavity and oropharynx lesions are staged as T4. CT can best assess cortical involvement of bone where findings such as cortical erosion, aggressive periosteal reaction, abnormal attenuation, and pathologic fractures indicate involvement (Figs. 4.6 and 4.12). MRI may also be used to assess osseous involvement although studies have shown a lower specificity for tumor involvement. MR imaging findings suggestive of osseous involvement include loss of normal low signal intensity cortex, replacement of high signal intensity marrow on T1-weighted images by intermediate signal tumor, and contrast enhancement of nerves, particularly the inferior alveolar nerve in the mandible (Fig. 4.10). However, it is important to be mindful of potential false positives such as artifacts (Fig. 4.23), recent dental extraction, radiation-induced fibrosis, and osteoradionecrosis. The presence of osseous involvement necessitates at least partial resection of the bone if the tumor is to be treated surgically.
3. *Neurovascular involvement*: A critical part of imaging evaluation in these cancers is to detect perineural spread along CN's XII and V3, the greater and lesser palatine nerves, and the posterior superior alveolar nerves. Imaging features suggestive of perineural spread include enlargement of the nerve on contrast-enhanced MR images and foraminal enlargement with replacement of normal fat within the neural foramen (Fig. 4.24). Although CT may demonstrate foraminal enlargement, MRI best detects perineural spread. The most commonly involved neurovascular bundles include the inferior alveolar nerve in cases of mandibular invasion (Fig. 4.25), the lingual neurovascular bundle in cases with involvement of the oral tongue and FOM (Figs. 4.13 and 4.15), and the greater and lesser palatine nerves

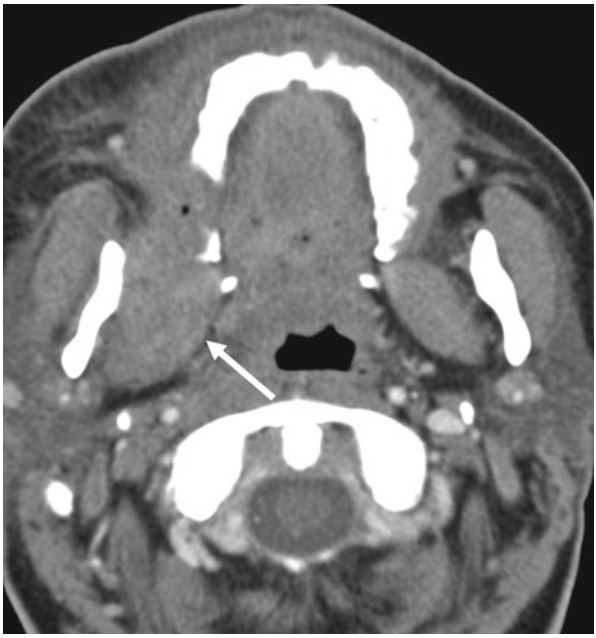

Fig. 4.23 Axial CT image in the same patient in Fig. 4.22 demonstrates invasion of the right medial pterygoid muscle (*arrow*)

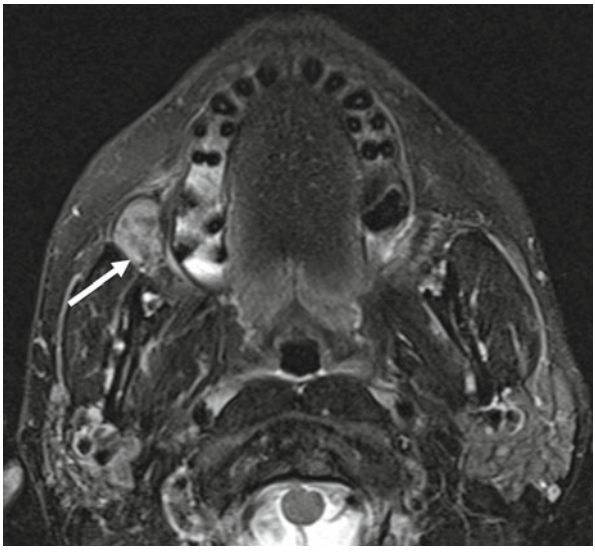

Fig. 4.24 Axial T2-weighted MR image with fat saturation demonstrates a T2- hyperintense mass (*arrow*) arising from the right buccal mucosa. Increased T2 signal within the right maxilla is secondary to artifact from dental hardware

when there is involvement of the hard palate (Fig. 4.16). Therefore, SCC involvement of these subsites requires evaluation for possible neurovascular spread.

4. *Evaluation of regional lymph nodes*: As with all head and neck SCC's, a thorough evaluation should be done for bilateral nodal disease, including presence of extracapsular spread and possible involvement of critical anatomic structures (Fig. 4.26). Cervical nodal imaging is covered in detail in Chap. 2.

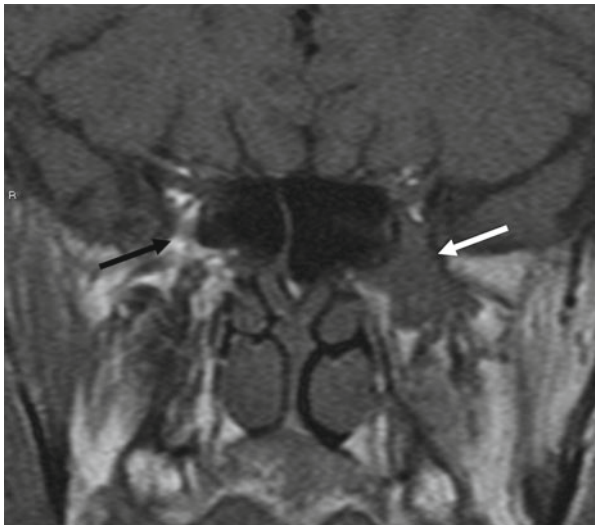

Fig. 4.25 Coronal T1-weighted MR image demonstrating perineural spread of tumor. There is replacement of the normal fat within the left pterygopalatine fossa (*white arrow*) with soft tissue. Compare with the normal appearance of the right pterygopalatine fossa (*black arrow*)

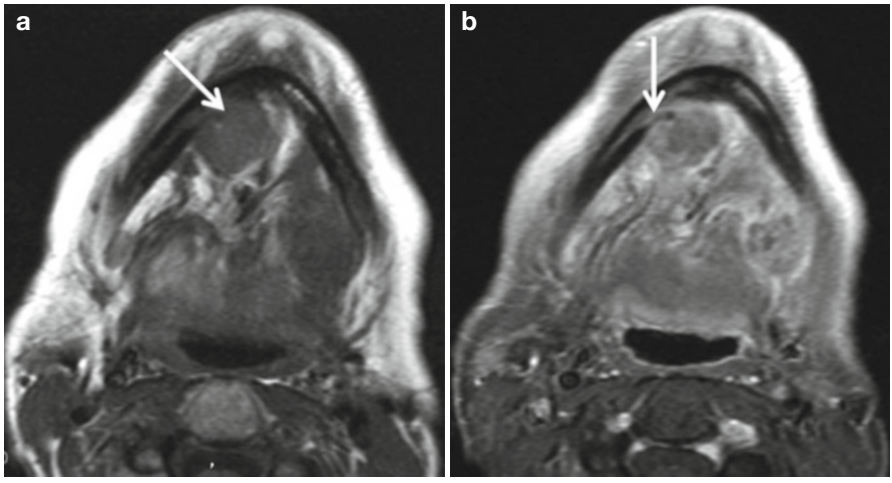

Fig. 4.26 Axial pre-contrast T1 (**a**) and post-contrast fat-saturated images (**b**) demonstrate a large recurrence within the flap with mandibular invasion and perineural extension along the right inferior alveolar nerve. Note loss of the predominant fat signal within the flap with mass-like enhancing soft tissue recurrent tumor within it (*white arrow*)

4.3.4 Posttreatment Imaging in Oral and Oropharyngeal Cancers

Treatment in OC/OP cancers involves surgery, radiation, and/or chemotherapy. An understanding and familiarity with the surgical techniques and with the expected post-radiation changes is essential in interpreting posttreatment scans. Imaging is targeted at identifying response to therapy and/or residual/recurrent tumor.

Although FDG PET-CT has a high sensitivity (80–100 %) for detection of residual and recurrent cancers and nodal disease after radiotherapy, its specificity is quite

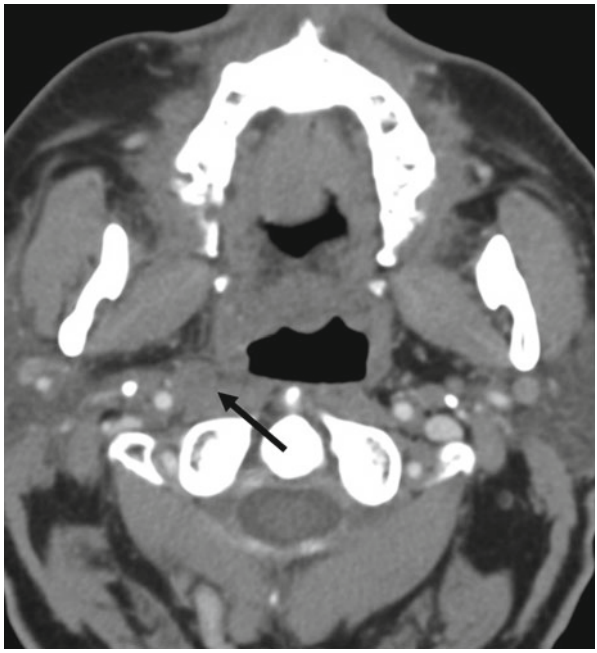

Fig. 4.27 Axial contrast-enhanced CT image with a right retropharyngeal lymph node (*black arrow*) in a patient with tonsillar SCC

low and variable (60–90 %). It is far better for detection of regional and distant recurrences than for local recurrence (Fig. 4.27). In the initial posttreatment setting, false positives are due to posttreatment inflammation or infection. Causes for false negatives are more nebulous; they may represent decreased perfusion because of radiation-induced vascular damage or a state of temporarily decreased glucose uptake, possibly due to depression of glucose transporters. The accuracy of FDG PET-CT improves markedly at 12 weeks or more after treatment, but the 12-week interval is considered too long for patients with disease persistence in whom surgical intervention is warranted. In such patients, a window of 4–8 weeks minimizes fibrosis and optimizes healing. Consequently, National Comprehensive Cancer Network (NCCN) guidelines currently recommend contrast-enhanced CT or MRI within 4–8 weeks of (chemo) radiotherapy in higher-risk patients or those with suspected disease persistence/progression.

Newer techniques such as perfusion CT and diffusion-weighted MR imaging are being used as adjuncts, though further studies are needed to validate results. Baseline posttreatment imaging is very helpful in many of these situations.

Curative surgical resection for locally advanced OC/OP cancers is frequently repaired using complex flap reconstructions for both cosmesis and function. Flaps can be pedicled (retaining native blood supply) or free (primary vascular pedicle detached and reanastomosed to local vasculature). The most common free flap used in OC/OP reconstruction is the radial forearm free flap, but a variety of others are used as well. The most common pedicled flap remains the pectoralis major; it is used in patients that are poor candidates for free tissue transfer or in cases where soft tissue bulk and/or improved vascularization are required within its anatomic range. When imaged over time, myocutaneous flaps demonstrate fatty atrophy and

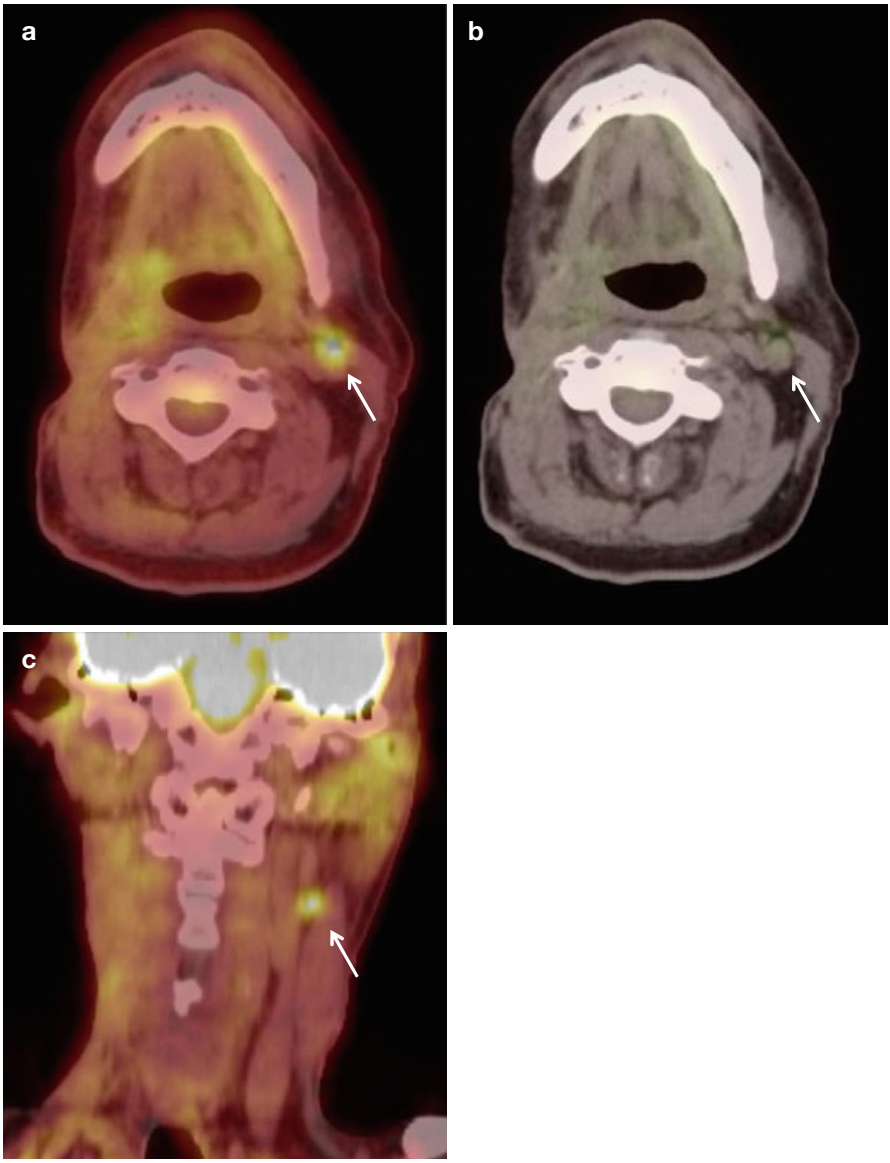

Fig. 4.28 PET-CT can play a very helpful role in posttreatment evaluation as in this case. Patient has had multiple surgeries and radiotherapy for a T2N3M0 lesion, with extensive postsurgical and RT changes; PET was specifically requested as CT imaging interpretation was difficult due to altered anatomy. Axial (**a**) and coronal (**b**, **c**) PET shows abnormal uptake in a left level II node, (*arrow* in **a**, **b** and **c**) consistent with residual nodal disease. Diffuse uptake in the right neck is secondary to posttreatment changes

decreased bulk due to denervation atrophy (Fig. 4.28). Consequently, any increase in bulk or any focally enhancing mass, particularly at the margin of the flap, is concerning of recurrent tumor (Fig. 4.29).

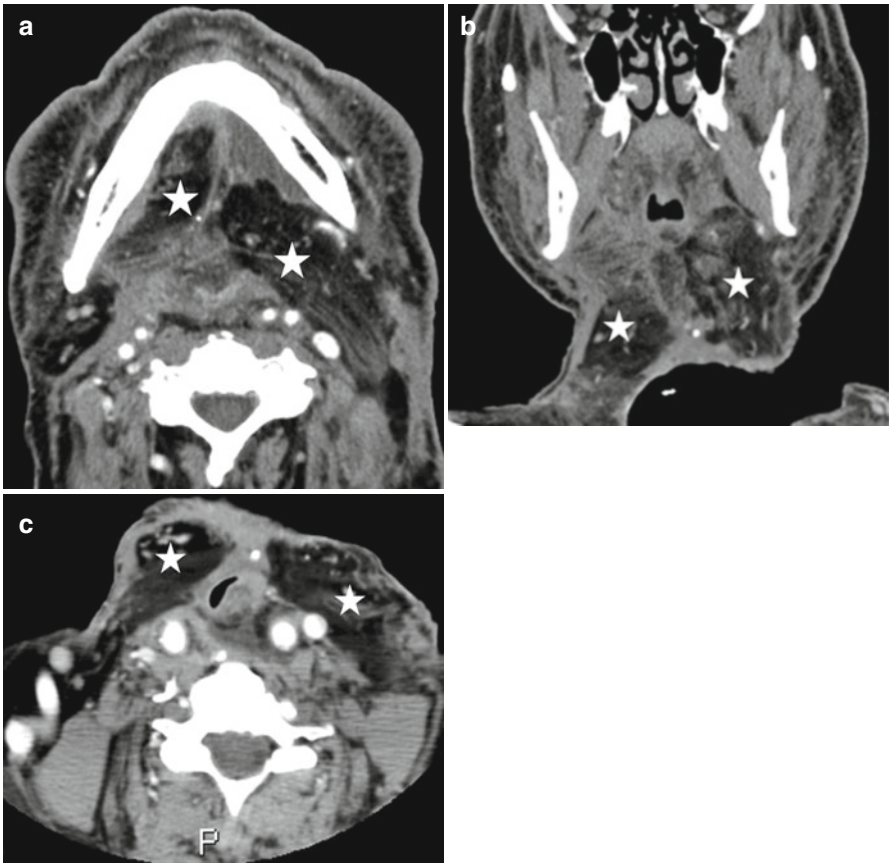

Fig. 4.29 A 51-year-old with floor of mouth cancer and extensive bilateral nodal disease status tumor resection and bilateral flap reconstruction. Six-month follow-up scans axial (**a**, **c**) and coronal (**b**) demonstrates bilateral pectoralis major myocutaneous flaps (*stars* in **a**, **b** and **c**) with changes of denervation atrophy (volume loss and fatty replacement)

Other postoperative changes include secondary infections, fistulas (Fig. 4.30), and abscesses as well as hematomas and seromas. Postsurgical changes of the various kinds of neck dissections are discussed in Chap. 2.

Radiation induces necrosis, mucosal changes, soft tissue fibrosis, and mandibular osteoradionecrosis in the local field (Fig. 4.31). Additionally, radiotherapy impacts other tissues such as brain, upper cervical spinal cord, and upper lungs. Head and neck radiologists should be accustomed to post-radiation changes. The early changes are very common and reversible and include findings of mucositis and skin desquamation. Late changes are more worrisome and include soft tissue necrosis, vascular complications, osteoradionecrosis, and secondary malignancies. Post-radiation changes can be easily identified on CT and MR imaging and include any combination of reticulation of the subcutaneous fat, edema in the retropharyngeal spaces, thickened skin and platysma, and increased enhancement within the

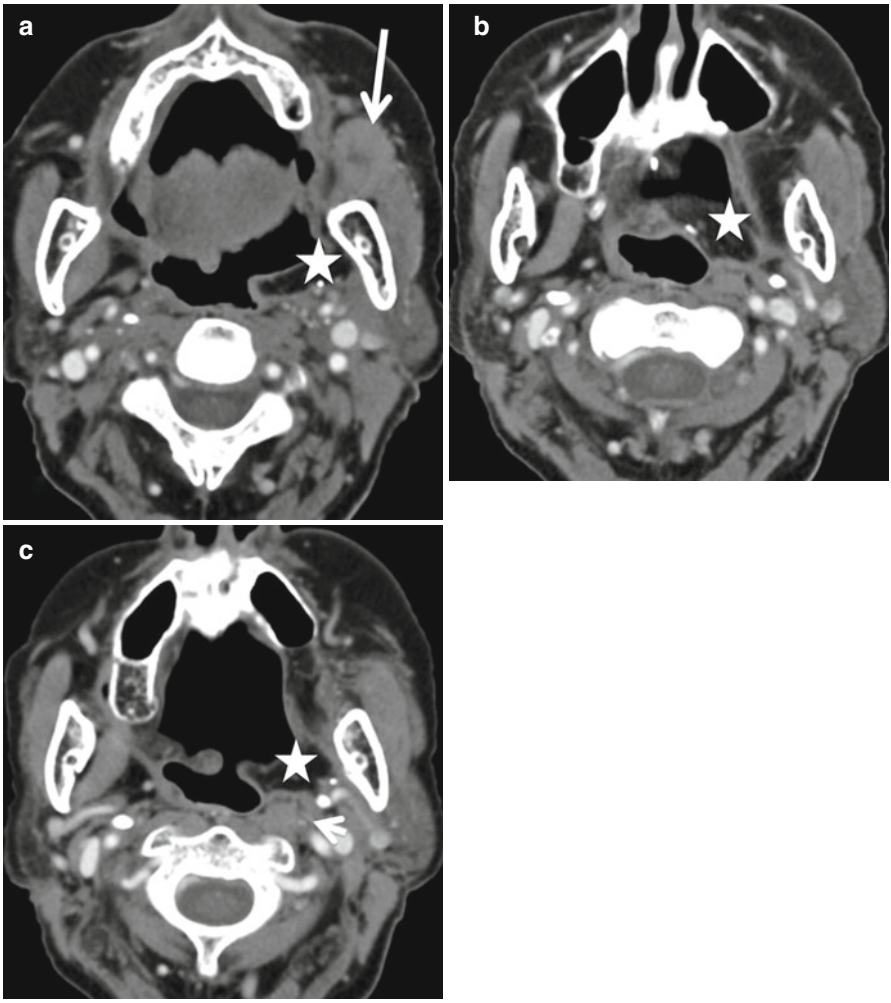

Fig. 4.30 A left buccal space recurrence in a 55-year-old with left oropharyngeal cancer status post-tumor resection and flap reconstruction. Axial CT images (**a**, **b** and **c**) show a heterogeneously enhancing mass (*arrow* in **a**) adjacent to the flap (*star* in **a**, **b** and **c**). Also note the pathological new left-sided retropharyngeal node (*smaller arrow* in **c**)

pharyngeal mucosa and the salivary glands (Fig. 4.32). Later changes include more fibrosis within the skin, platysma, and deeper soft tissue structures as well as atrophy of the salivary glands.

4.4 Other Oral and Oropharyngeal Neoplasms

The presence of lymphoid tissue in the tonsils and BOT as well as the presence of minor salivary gland tissue throughout the OC/OP accounts for the spectrum of neoplasms seen in addition to carcinomas, which principally includes salivary

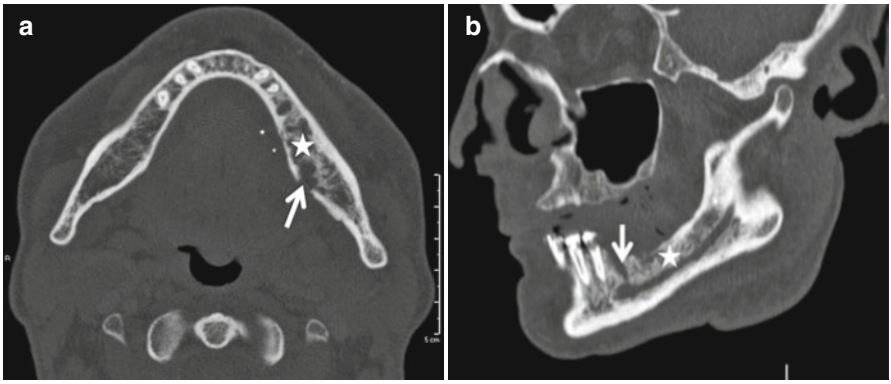

Fig. 4.31 Axial (**a**) and sagittal (**b**) CT images in a patient treated 2 years prior with radiation, for left-sided tongue cancer. Findings of mandibular osteoradionecrosis are seen with loss of lingual cortex (*arrow*) and resorption of the trabeculae (*star*)

tumors and lymphomas; these are reviewed in Chaps. 1 and 9. Although a variety of mesenchymal and other neoplastic lesions can involve the OC/OP, they are quite rare and most have no distinct imaging features. Boxes 4.4 and 4.5 summarize both the neoplastic and nonneoplastic lesions within the sublingual and submandibular spaces.

4.5 Nonneoplastic Lesions

Nonneoplastic lesions within the OC/OP run the whole gamut. Developmental and congenital lesions including benign cysts (e.g., ranula (Fig. 4.33), thyroglossal ducts remnants, dermoids, and epidermoids) and vascular malformations. Most of these have been discussed in Chaps. 9, 10, and 11. Infectious and inflammatory lesions, predominantly odontogenic in origin, represent the vast majority of nonneoplastic processes and are discussed below. Jaw lesions are covered in detail in Chap. 13.

4.5.1 Inflammatory Lesions of the Oral Cavity and Oropharynx

The OC/OP is frequently involved with infectious/inflammatory processes, secondary to odontogenic or tonsillar infections or to salivary gland obstruction. Odontogenic disease is the most frequent source of oral cavity infection in adults, whereas the palatine tonsils are the most frequent source in children and young adults.

4.5.2 Odontogenic Infections

Odontogenic infections can be dental or periodontal in origin with resultant periapical abscess. These can then spread to maxillary sinus, masticator space, buccal

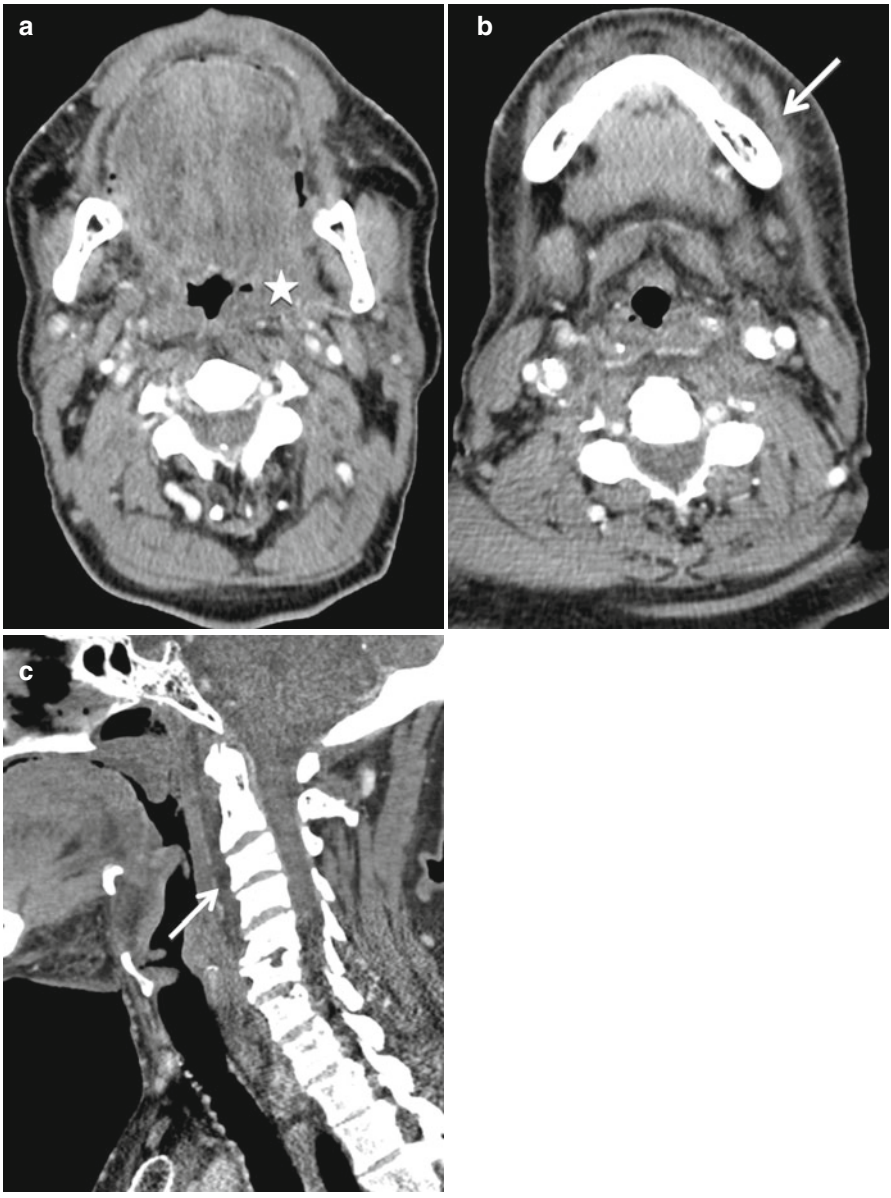

Fig. 4.32 Post-radiation changes in a patient with left-sided tonsillar tumor (*star* in **a**) show expected changes of soft tissue thickening and stranding, including platysma thickening and retropharyngeal edema. Figure (**a**) is the axial pretreatment scan, while figures (**b**, **c**) are axial posttreatment scans

Box 4.4. Sublingual Space/Floor of Mouth Lesions

Cystic lesions	Ranula (simple or plunging), dermoid and epidermoid cysts
Infectious/inflammatory processes	Phlegmon-cellulitis, abscess, submandibular duct stenosis, and calculi
Developmental	Lingual thyroid
Vascular malformations	Arteriovenous malformations (high and low flow), hemangiomas, lymphatic malformations, venous and mixed venolymphatic malformations
Neoplastic lesions	Benign lesions (lipomas, nerve sheath tumors, benign mixed tumor) and malignant tumors (squamous cell carcinomas and salivary gland tumors)
Pseudolesion	Tongue atrophy from hypoglossal palsy

Box 4.5. Submandibular Space Lesions

Cystic lesions	Thyroglossal duct cyst, dermoid and epidermoid cyst, second branchial cleft cyst
Inflammatory processes	Phlegmon-cellulitis, abscess, reactive adenopathy
Submandibular diseases	Stenosis and calculi, mucocele
Vascular malformations	Arteriovenous malformations (high and low flow), hemangiomas, lymphatic malformations, venous and mixed venolymphatic malformations
Neoplastic lesions	Benign lesions (lipomas, nerve sheath tumors, benign mixed tumor) and malignant tumors (squamous cell carcinomas and salivary gland tumors)
Pseudolesions	Secondary to mandibular nerve atrophy, small mylohyoid, anterior belly of digastric

space, and sublingual/submandibular spaces (Fig. 4.34). The attachment of the mylohyoid muscle to the mylohyoid ridge dictates the spread to sublingual and submandibular spaces. Infections arising in the anterior mandibular teeth (incisors, canines, premolars, and first molars) spread to the sublingual space due to their position above the mylohyoid line (Fig. 4.35), whereas those arising in the second and third molars spread to the submandibular space as their apices lie below the mylohyoid line. Imaging findings include edematous changes in the muscles, salivary glands, and soft tissues with obscurations of fat planes with stranding. On

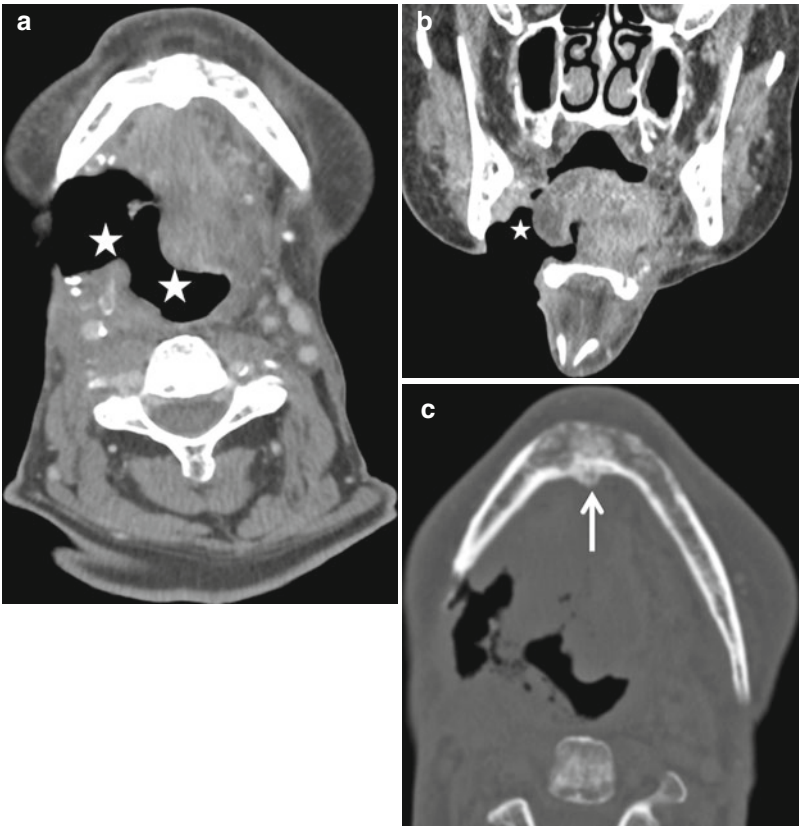

Fig. 4.33 Axial (**a**) and coronal (**b**, **c**) CT images of a patient with extensive right-sided neck surgery and radiation for recurrent oropharyngeal cancer with a large right side pharyngocutaneous fistula (*star* in **a**, **b**). Also note the changes of osteoradionecrosis within the mandible (*arrow* in **c**)

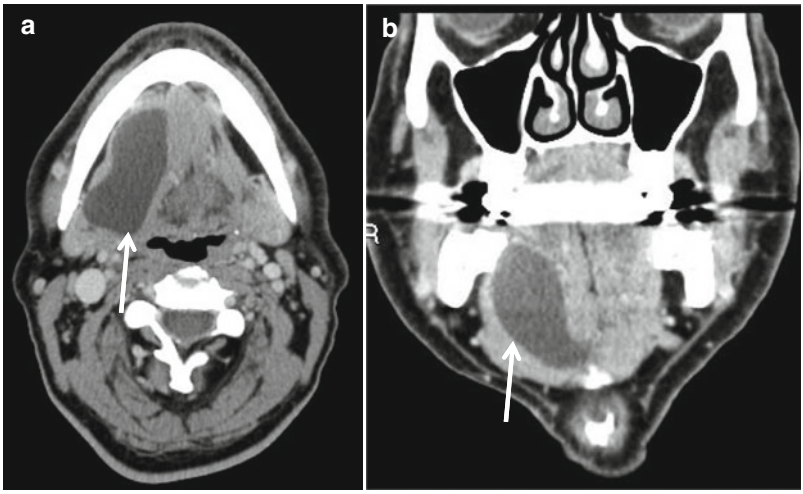

Fig. 4.34 A well-defined hypodense lesion (*arrow*) is seen in these axial (**a**) and coronal (**b**) CT scans, centered within the right sublingual space, consistent with a ranula

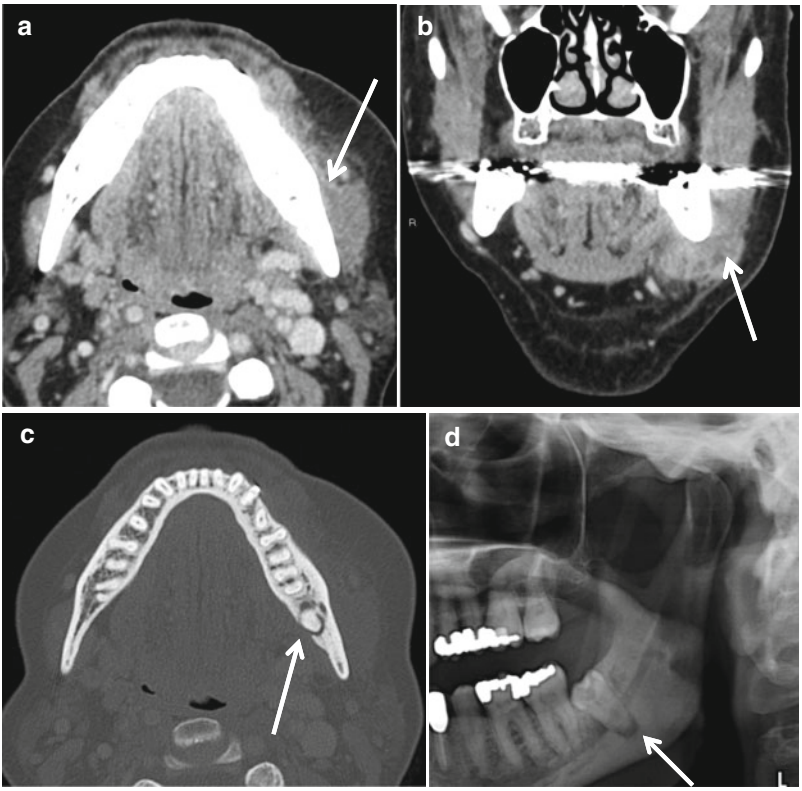

Fig. 4.35 Axial (**a**)- and coronal (**b**)-contrasted CT images in a patient with left submandibular abscess (*arrow* in **a** and **b**). The bony windows (**c**) demonstrate left mandibular molar periodontal lucency (*arrow*) with loss of lingual cortex. The periodontal lucency (*arrow*) can also be well identified on the panorex view (**d**)

contrast-enhanced CT, one can identify changes consistent with phlegmon, with more organized rim-enhancing abscesses becoming more obvious later in the course of the illness.

4.5.3 Infections of Salivary Gland Origin

Sialadenitis and related sialolithiasis are discussed in detail in Chap. 9.

4.5.4 Tonsillar/Peritonsillar Infections, Peritonsillar Abscess

Routine imaging is not performed in acute tonsillitis, which is very common in children. Uncomplicated tonsillitis appears as edematous, enlarged palatine tonsils. Imaging in tonsillitis may be warranted patients with potential complicating features such as progressive difficulty in swallowing, trismus, ear pain, torticollis, and

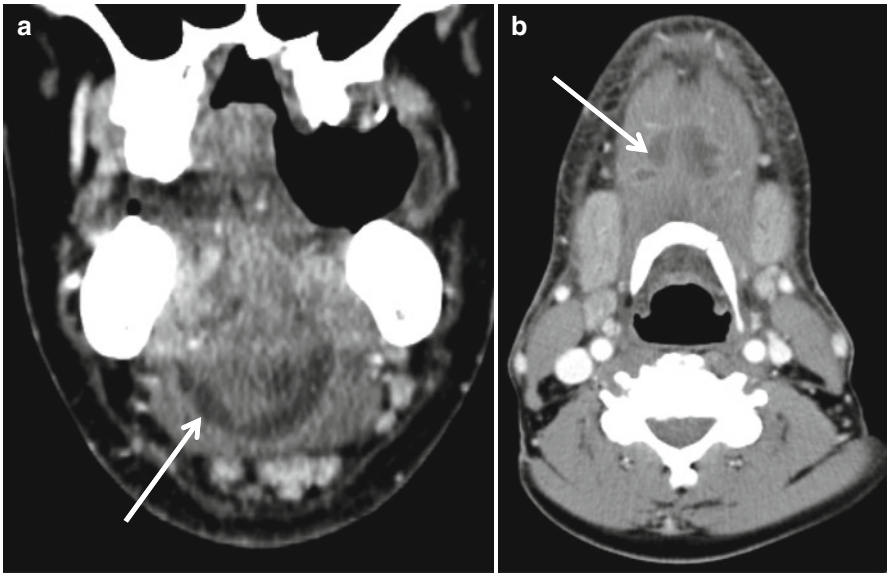

Fig. 4.36 Coronal (**a**) and axial (**b**) post-contrast CT scan images demonstrate a well-defined rim-enhancing abscess (*arrows*) in the sublingual space. Note the abscess location in between the tongue superiorly and the mylohyoid muscle inferiorly. Multiple enhancing reactive nodes are present

bulging of the pharyngeal wall, concerning for a retropharyngeal abscess. Routine peritonsillar abscesses are diagnosed clinically and do not require imaging; they occur when infection extends outside the tonsillar capsule and into the lateral pharyngeal space between the tonsillar capsule and superior constrictor muscle. Peritonsillar abscesses appear as rim-enhancing collection, limited laterally by the superior constrictor muscle. However, they may extend into the parapharyngeal or retropharyngeal spaces, which must be mentioned in the radiology report, as this can affect the surgical approach (Figs. 4.36 and 4.37).

4.5.5 Suppurative Lymphadenitis

Level Ia and Ib lymph nodes can be affected by infectious processes but rarely undergo necrosis to form an intranodal abscess. This is most commonly seen in children due to *Staphylococcus aureus* infection and is known as suppurative adenitis.

4.5.6 Necrotizing Fasciitis

Necrotizing fasciitis, which can affect any part of the body, can also involve the superficial and deep tissues of the neck. It is a rare, severe, rapidly progressive bacterial infection, which can destroy tissues across fascial planes, including skin,

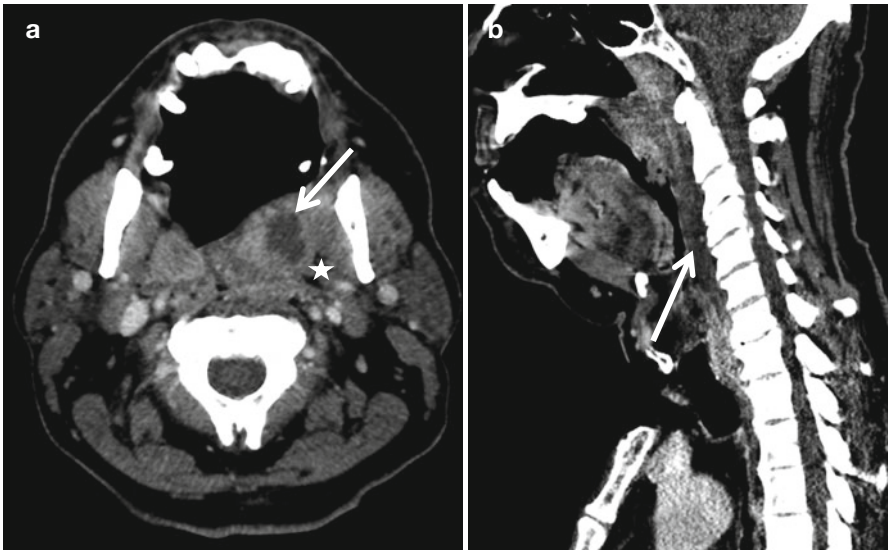

Fig. 4.37 Axial (**a**) and sagittal (**b**) contrast-enhanced CT shows low-density irregular left intra/peritonsillar abscess (*white arrows* in **a**) with minimal stranding in the left parapharyngeal space (*star* in **a**). The right tonsils demonstrate mildly striated enhancement, which is suggestive for inflammation. Note the large sympathetic effusion in retropharyngeal space (*white arrow* in **b**)

muscles, and other soft tissues. A variety of aerobic and anaerobic bacteria can be involved. On imaging, a combination of diffuse cellulitis, fasciitis, and myositis of the superficial and deep soft tissues is seen, sometimes with small pockets of air.

4.5.7 Ludwig's Angina

Ludwig's angina is a rare condition and represents a head and neck therapeutic emergency. It involves a diffuse life-threatening infection of the sublingual space with associated severe sublingual and lingual edema resulting in expansion and retropulsion of the tongue with airway obstruction. Infection often extends to the submandibular spaces with clinical findings of dysphagia, trismus, and induration of the upper neck soft tissues. Most of these are odontogenic in origin, usually due to an infection of the third molar or the gums surrounding a partially erupted third molar, and caused by *Streptococcus* species. On cross-sectional imaging, there is diffuse infiltration and edema centered in the sublingual region that is phlegmonous in appearance without a discrete abscess. The submandibular spaces, submandibular glands, and other immediate fascial spaces are frequently involved. Given the potential for airway compromise, and other serious complications (jugular thrombophlebitis, empyema, mediastinitis, etc.), this process requires urgent intervention. On imaging, attention should be paid to airway patency and the identification of any drainable abscess.

4.5.8 Other Lesions

Various other lesions, including congenital lesions and vascular malformations, are discussed elsewhere in this book (Chap. 11).

4.6 The Surgeon's Perspective

4.6.1 Oral Cavity Lesions

As in other areas of the head and neck, imaging of the OC/OP is crucial for accurate diagnosis, staging, and therapeutic planning. When considering OC lesions, superficial noninvasive lesions can be managed without imaging, but all invasive lesions should undergo head and neck CT or MRI. OC SCC, particularly oral tongue, FOM, and buccal cancers, have a high rate of occult cervical nodal metastases and continue to have relatively poor survival despite aggressive therapy. Since all patients with N+ disease are at least stage III, imaging evaluation often differentiates between early stage (I/II) and late stage (III/IV) cancers. This is crucial because, while single modality therapy (e.g., surgery alone) may be an option for early stage OC cancers, advanced disease is always treated with a multimodal approach (e.g., surgery and postoperative radiotherapy ± chemotherapy).

It is important to have completed a thorough clinical examination when reviewing OC imaging, since some imaging findings can be misleading. For instance, a lesion that is clearly isolated to the lateral tongue on physical exam with the tongue protruded may appear on imaging to involve the FOM or lingual gingiva of the mandible since the tumor abuts these areas with the tongue at rest in the mouth. Similarly, a recently extracted tooth may leave behind ragged, eroded bone on imaging but may be clearly free of tumor on physical exam; while it is important to note bony erosion on imaging, it is equally important that this be clearly associated with the cancer and not present for another reason.

OC imaging is particularly important for determining depth of invasion and bony involvement. On physical exam, deep infiltrative invasion of the tongue may not be palpable but may be readily recognized on CT or MRI. While tumors that are fixed to the periosteum on physical exam have a high risk of bone invasion, this cannot be clearly delineated without imaging. As a general rule, tumors that abut the periosteum can be managed surgically with periosteal resection without bone removal. In this case, a section of periosteum should undergo intraoperative pathological evaluation, and if positive, a rim mandibulectomy should be performed. In cases where the periosteum is clearly invaded but the bone is pristine on imaging, a rim mandibulectomy should be performed. If the bony cortex is breached by tumor, the patient should undergo a segmental mandibulectomy. Many surgeons submit bone marrow at the cut edges of bone for frozen section analysis at the time of resection. While not infallible, this is the best approach to confirming negative bony margins intraoperatively since the bone itself cannot be assessed. Given that these approaches dramatically change the extent and duration of surgery and the reconstructive

approach, it is crucial to have as much information as possible before proceeding with surgery.

While surgical reconstructive approaches are well beyond the scope of this text, it behooves the head and neck radiologist to be comfortable with these in terms of the postoperative imaging appearance. Since they are often unique, good communication between the surgeon and the radiologist as to the details of the surgical intervention is necessary so that the imaging report does not reflect a normal reconstructive element as concerning for recurrence. Preoperative imaging is often essential for reconstructive planning, particularly when bony reconstruction will be required, particularly as new imaging-based computer-assisted reconstructive planning tools become more commonplace.

4.6.2 Oropharynx Lesions

For OP SCC, imaging is perhaps even more important. BOT and tonsil cancers are difficult to evaluate by physical exam in the clinic and even under general anesthesia. When tonsil cancers are mobile on exam, they are almost always T1/2 and surgically resectable via transoral approaches, which are becoming more popular as they have the potential to allow for reduced use of the chemotherapy and/or radiotherapy. This is important in terms of improving long-term morbidity, particularly in an era where most new OP cancers are HPV related, with, in general, younger, nonsmoking patients. To consider a transoral surgical approach, the surgeon must understand the extent of the tumor and its relationship to the carotid vessels, as well as the relative position of these vessels to the pharyngeal walls. Superior extent of tonsil tumors should be assessed carefully since soft palate resection will have significant functional consequences for the patient and reconstruction may be required. For BOT tumors, careful consideration is given to the lingual vascular pedicles; tumors that cross the midline are generally considered poor candidates for transoral surgery since both vascular pedicles are likely to be ligated during the procedure, resulting in necrosis of the distal tongue. Additionally, BOT tumors that extend into the preepiglottic and/or paraglottic spaces require at least supraglottic laryngectomy for complete surgical removal; these findings may push treatment planning toward primary chemoradiotherapy.

Accurate staging is also important for nonsurgical treatment planning for OP cancers. Again, early stage lesions can undergo unimodality therapy (e.g., radiotherapy alone), but advanced cancers generally require multimodality therapy (e.g., chemoradiotherapy). Mid-stage cancers (e.g., T1N1 tonsil) may be considered for unimodality therapy unless extracapsular spread (ECS) is present around the metastatic cervical node, and thus the imaging report should always comment on the present or absence of ECS. BOT tumors routinely require treatment of both the left and right cervical nodal basins. Imaging is also commonly obtained for infectious processes in the OP. However, this is rarely necessary. Tonsillar cellulitis and peritonsillar abscess are diagnosed clinically and can almost always be managed without imaging. In settings where these commonly present (emergency departments,

student health organizations), primary providers should be encouraged to obtain clinical consultation with an otolaryngologist or other experienced provider rather than relying on imaging, which, in this case, involves unnecessary expense and radiation exposure for the patient.

In similar clinical settings, Ludwig's angina is a common question but is rarely seen. In most cases, these are perimandibular infections that result in extensive submandibular swelling with edema and possibly abscess inferior to the mylohyoid muscle. In true cases of Ludwig's angina, significant swelling is present in the floor of mouth due to cellulitis in the sublingual space superior to the mylohyoid muscle. This results in superior and posterior displacement of the tongue with OP compression and airway obstruction. When this situation presents, securing the airway is paramount and takes priority over CT imaging. In the unexpected situation where these findings are present but not advanced enough to cause airway obstruction, the radiologist should communicate rapidly to the requesting physician with a recommendation for acute airway evaluation.

Further Reading

Mukherji SK, Weissmann JL, Holliday RA (2003) Pharynx. In: Som PM, Curtin HD (eds) Head and neck imaging, 4th edn. Mosby, St Louis

Smoker WRK (2003) The oral cavity. In: Som PM, Curtin HD (eds) Head and neck imaging, 4th edn. St Louis Smoker WRK, Mosby